Eur J Appl Physiol (2003) 88: 317–338
DOI 10.1007/s00421-002-0676-3

REVIEW ARTICLE

Alois Mader

Glycolysis and oxidative phosphorylation as a function of cytosolic phosphorylation state and power output of the muscle cell

Accepted: 12 June 2002 / Published online: 22 November 2002

Abstract A mathematical description of the regulation of ATP production in muscle cells is presented whereby the activity of OxP can be calculated as a function of (1) free [ADP] as the substrate and (2) a second driving force $\Phi\Delta G$ (kilojoules per mole) resulting from the difference of free energy $\Delta G_{ox,ap}$ (kilojoules per mole) – $\Delta G_{ATP,cyt}$ (kilojoules per mole). In turn, the term $\Delta G_{ox,ap}$ results from the proton motive force and the generation of ATP in the matrix space including the ATP-ADP exchange, whereas the phosphorylation state of the CHEP-sytem is described by $\Delta G_{ATP,cyt}$. Regulation of glycolysis is calculated as a function of free [ADP] and [AMP] at the level of PFK. The PFK is inhibited by a decreasing pH resulting from lactate accumulation. The ATP/PCr equilibrium of the CHEP-system is calculated by algebraic equations. The dynamic behaviour of the metabolic control of ATP production as a function of ATP consumption is calculated by a system of two 1st-order non-linear differential equations, including a time delay considering oxygen transport. Lactate distribution and elimination is calculated using a two-compartment model with an active lactate producing, and a passive, space including lactate elimination by combustion. The simulation of the dynamics of energy metabolism of muscle cells is performed by the stepwise solution of the differential equations with a 5th-order Runge-Kutta-Fehlberg-routine. Examples of various applications of the simulation of the dynamics of energy supply demonstrate the qualitative and quantitative congruence to the behaviour of metabolic processes in experiments during rest, exercise and recovery.

Keywords Regulation of oxidative phosphorylation and glycolysis · Mathematical model · Computer simulation of energy metabolisms · Cytosolic ATP/PCr equilibrium

Symbols and abbreviations

$\Delta G_{ATP,cyt}$	Current free energy of the CHEP system (at rest –58 and –65 kJ·mol^{-1})
$\Delta G_{ATP,mit}$	Current free energy of the inner mitochondrial ATP/ADP system build up by Δp and the F_0F_1-ATPase
$\Delta G_{ox,ap}$	Current free energy build up by $\Delta G_{ATP,mit}$ and the ATP^{-4}/ADP^{-3} translocase
$\Delta G_{ox,const}$	–72.5 kJ·mol^{-1}, Arbitrarily set maximum of free energy of $\Delta G_{ox,ap}$ used in the simulation model
ΔG_0	Standard free energy of the [ATP]/[PCr] system, –30.6 kJ·mol^{-1}
Δp	Mitochondrial proton motive force (pmf), about –220 mV, equivalent to about –21.7 kJ·mol^{-1} generated by the respiratory chain
$\Delta p'$	pmf expressed in kilojoules per mole
$\Phi\Delta G_{ADP}$	Force equivalent of free [ADP] resulting from $\Delta G_{ox,ap}$–$\Delta G_{ATP,cyt}$, being the driving force necessary to sustain the flow of ATP from inside the mitochondrian to the cytosol
$\Delta\psi$	Mitochondrial transmembrane electrical potential, about –160 mV
Σ[A]	Sum of concentrations of cytosolic adenosine phosphate compounds (S[A] = [ATP] + [ADP] + [AMP]), millimoles per kilogram

This paper is dedicated to Professor Doctor Doctor h.c. Wildor Hollmann.
Parts of this manuscript were presented at the 1999 American College of Sports Medicine Symposium entitled Exercise lactate levels: simulation and reality of aerobic and anaerobic metabolism, chaired by Serge P. von Duvillard. For other contributions to the Symposium see Eur J Appl Phsyiol (2001) 86:3–16, articles by S.P. von Duvullard, A. Bonen and C. Juel.

A. Mader
Institute for Cardiology and Sports Medicine,
German Sports University – Cologne,
Carl Diem Weg 6, 50933, Cologne, Germany
E-mail: MaderAG@t-online.de
Tel.: +49-2234-360066
Fax: +49-2234-360066

$\tau_{\dot{V}O2}$	used as a refence for an approximate characterisation of the response delay of a non 1st-order system by the time constant (or delay time) of a first order system. The time behaviour of a 1st-order system is described by: $a = e_0 \cdot (1 - e^{-t/\tau})$ where a is the response amplitude at time t after the start, and e_0 is the final amplitude approached after an infinite time t. The $\tau = e_0 \cdot (1–1/e)$ (approximately $0.666 \cdot e_0$)
$\Sigma[C]$	Sum of concentrations of compounds available to store phosphate bond energy in the cytosol ($S[C] = [PCr] + [P]_i$), millimoles per kilogram
[ADP]	Concentration of cytosolic adenosine diphosphate, millimoles per kilogram wet mass, or millimoles per litre
$[ADP]_{mit}$	Concentration of inner mitochondrial adenosine diphosphate, matrix space, millimoles per litre
[AMP]	Concentration of adenosine monophosphate, millimoles per kilogram wet mass, or millimoles per litre
[ATP]	Concentration of cytosolic adenosine triphosphate, millimoles per kilogram wet mass, or millimoles per litre
$[ATP]_{mit}$	Concentration of the inner mitochondrial ATP, matrix space, millimoles per litre
ATP^{-4}/ADP^{-3}-translocase	protein complex located in the inner mitochondrial membrane which transfers ATP (built up by the F_0F_1-ATPase) from matrix to the cytosol in exchange for ADP. The ATP^{-4} and ADP^{-3} are transferred in ionic form; so ATP is 4 times and ADP is 3 times negatively charged
b_{Pow}	Rate of GP consumption per watt, millimoles per kilogram per second per watt
$b_{v,la}$	Transformation coefficient of v_{la} into $v_{GP,vla}$, about 1.4 mmol lactate·$mmol^{-1}$ GP
$b_{\dot{V}O2}$	Transformation coefficient of $\dot{V}O_2$ into $v_{GP,\dot{V}O2,a}$, about 4.3 $mlO_2 \cdot mmol^{-1}$ GP
Ca^{2+}	Calcium ion
CHEP	Cytosolic high energy phosphate-
CK	Creatine kinase
cP_E	Arbitrary conversion factor
[Cr]	Concentration of creatine, millimoles per kilogram muscle
CS	Computer simulation
d_{buff}	Coefficient equal to the mean buffering capacity of skeletal muscle
$d[GP]/dt$	Rate of change of the sum of [ATP] + [PCr], millimoles per kilogram per second
$d[GP]_{\dot{V}O2,a}/dt$	Rate of change of instantaneous oxidative GP production
$d[la^-]_b/dt$	Rate of change of lactic acid concentration (millimoles per litre per second) in the passive lactate producing compartment (blood)
$d[la^-]_m/dt$	Rate of change of lactic acid concentration (millimoles per litre per second) in the active lactate producing compartment (muscle)
$dv_{GP,\dot{V}O2,a}/dt$	Rate of change of $v_{GP,\dot{V}O2,a}$
$d\dot{V}O_{2,a}/dt$	Rate of change of $\dot{V}O_{2,a}$
E	Energy flow, watts
F_0F_1-ATPase	protein complex located in the inner mitochondrial membrane which harvests the energy of 3 protons to build up one molecule of ATP. The energy transferred by the move of the protons through the F_0 proton channel results from the pmf build up across the inner mitochondrial membrane. The ADP binding of the F_1-complex leads from the *open* to the *low* state where ADP is weakly bound. The move of H^+ from the cytosolic to the matrix side builds up the *tense* state until $G_{ATP,mit}$ is achieved and ATP is released from the F_1-complex
$F_{\Delta G}$	Factor which adjusts current power output [$F_{\Delta G} \cdot$E(watts per kilogram)] in relation to $\Delta G_{ATP,cyt}$
[GP]	Sum of concentrations of high energy phosphate compounds ([GP] = [ATP] + [PCr]), millimoles per kilogram
$[H^+]$	Hydrogen ion concentration
K_1	Coefficient relating rate of diffusion of lactate from muscle in terms of $[la^-]_b$ given in Eq. 31
$k_{el,ox}$	50% Activity rate constant of oxidative lactate elimination by combustion, as a function of lactate concentration
Km(0.5)	Common expression for the 50% rate constant of OxP. Equivalent to $v_{ss}/v_{max} = 0.5$
ks_1	50% Activation rate constant of Eq. 13 of OxP related to $\dot{V}O_{2max}$
ks_{1DG}	From -0.65×10^{-4} to $-0.95 \times 10^{-4} \cdot mol^{-1}$ free [ADP] per joules per mole free energy of the CHEP system
ks'_1	Hill coefficient of 50% activity of Eq. 9 of OxP related to $\dot{V}O_{2max}$
ks_2	50% Activation rate constant of glycolysis mainly due to PFK activation, [ADP] and [AMP] as activating factors

ks_3	50% Inhibition rate constant of glycolysis due to PFK inhibition by decrease of pH_m
$k_{\dot{V}O2}$	reciprocal of $t_{\dot{V}O2}$, per second
$[la^-]$	Concentration of lactate, millimoles per litre
$[la^-]_b$	Concentration of lactate in blood, millimoles per litre
$[la^-]_m$	Concentration of lactate in muscle, millimoles per litre
$[la^-]_{ss}$	Steady state concentration of lactate (millimoles per litre) during an equilibrium of lactate production and oxidative lactate elimination ($0 = v_{la,ss,pH} - v_{la,ox}$)
M_1	Hydrogen ion dependent creatine kinase equilibrium constant
M_2	Hydrogen ion independent creatine kinase equilibrium constant $1.66 \times 10^9 \cdot mol^{-1}$
M_3	Adenylate kinase equilibrium constant, range $0.85–1.15 \cdot mol^{-1}$
Mg^{2+}	Magnesium ion
$mval \cdot l^{-1}$	Expression for bases or acids of substances having an ionic dissociation in H_2O whose concentration is given in $mmol \cdot l^{-1}$. The unit mval expresses the ionic strength of the acid base status of blood and tissues
NAD^+	Nicotinic adenine dinucleotide (oxidized form)
NADH	Nicotinic adenine dinucleotide (reduced form)
nox	Exponent of the Hill equation for calculating the rate of OxP as a function of free [ADP]
OxP	Oxidative phosphorylation
PCO_2	Partial pressure of carbon dioxide (millimetres of mercury) at the tissue level
[PCr]	Concentration of phosphocreatine (PCR), millimoles per kilogram muscle
PDH	Pyruvate dehydrogenase
PFK	Phosphofructokinase
pH	$-\log_{10}[H^+]$
pH_m	Intracellular cytosolic pH
$[P]_i$	Concentration of free inorganic phosphate. millimoles per kilogram muscle, or millimoles per litre
PK	Pyruvate kinase
pmf	Proton motive force
^{31}P-NMR	^{31}Phosphorus nuclear magnetic resonance spectroscopy
P/O quotient	Relationship between the gain of high energy phosphate bonds and the H_2O produced. Typical value about 2.6
R	The gas constant, 2.0×10^{-3} kcal·mol^{-1}
RQ	Respiratory quotient
T	The absolute temperature Kelvin (C + 273)
$t_{\dot{V}O2}$	Time constant(seconds)of the rise of $\dot{V}O_2$ from the beginning of exercise, and during a period of constant load
$v_{GP,\dot{V}O2,a}$	Rate of oxidative rephosphorylation expressed in terms of [GP], millimoles per second per kilogram
$v_{GP,v,la}$	Rate of glycolytic rephosphorylation expressed in terms of [GP], millimoles per second per kilogram
$v_{GP,E}$	Power output expressed in terms of rate of GP consumption during contraction, millimoles per second per kilogram
$v_{GP,rest}$	Power output expressed in terms of rate of GP consumption at rest, millimoles per second per kilogram
v_{la}	Rate of lactic acid formation, millimoles per second per kilogram
$v_{la,max}$	Maximal rate of glycolysis expressed as rate of lactic acid formation, millimoles per second per kilogram
$v_{la,max,pH}$	pH Dependent maximal rate of glycolysis, expressed as rate of formation of lactic acid, millimoles per second per kilogram
$v_{la,ox}$	Rate of lactate elimination by oxidation, millimoles per minute per kilogram
$v_{la,ox,b}$	Rate of lactate elimination by oxidation (millimoles per minute per kilogram) in the passive compartment (blood)
$v_{la,ox,m}$	Rate of lactate elimination by oxidation (millimoles per minute per kilogram) in the active compartment (muscle)
$v_{la,ss}$	Steady-state rate of gross lactic acid (pyruvate) formation at pH above 7.4, $mmol \cdot s^{-1} \cdot kg^{-1}$
$v_{la,ss,pH}$	The pH dependent steady-state gross rate of formation of lactic acid, millimoles per second per kilogram
V_{mit}	Mitochondria volume, millilitres
V_{rel}	Quotient $\%V_m/\%V_b$, the volume of active lactate producing space (m, muscle, about 30% of total body volume) divided by the volume of the passive space (b, blood, about 15% of total body volume) available for lactate distribution during work and rest. Active and passive spaces together constitute between 35% and 50% of total body volume
1.35	Factor which relates muscle water space to active muscle mass (about 0.72)

$\dot{V}O_2$	Oxygen uptake, millilitres per minute or, millilitres per minute per kilogram body mass
$\dot{V}O_{2,a}$	Current $\dot{V}O_2$, millilitres per second per kilogram muscle
$\dot{V}O_{2,a,rest}$	Current $\dot{V}O_2$ at rest, millilitres per second per kilogram muscle
$\dot{V}O_{2max}$	Maximal oxygen uptake, millilitres per second per kilogram muscle or body mass
$\dot{V}O_{2max,ap}$	Simulated exponential increase in oxygen uptake, approaching the actual oxygen uptake, millilitres per second per kilogram muscle or body mass
$\dot{V}O_{2,ss}$	Steady state of $\dot{V}O_2$, millilitres per second per kilogram muscle mass wet weight
watts	Power, joules per second

Introduction and the general aspects of the regulation of the ATP producing reactions

The maintenance of a state of high phosphorylation of the CHEP-system and maintenance of the metabolic rate of ATP production is essential for the life of a cell; this is achieved using feedback control which adjusts the activity of the rephosphorylating processes to the instantaneous rate of dephosphorylation. There has, however, been disagreement concerning the explanation of the regulation of OxP in vivo for about 20 years. The regulation of the activity of OxP in vivo at a cellular level is believed to be different from that occurring in vitro (Balaban 1990; Brown 1992; Hochachka and Matheson 1992; Hochachka and McLelland 1997). The in vivo experimental results show that there is a gap between the flow rate of OxP, as obtained by the *Michaelis-Menten* (MM)-*type kinetics* as a function of the calculated free [ADP], and the experimental observations of the rate of OxP (Balaban and Heineman 1989; Connett 1988; Connett and Honig 1989; Heineman and Balaban 1990; Kantor et al. 1986; Katz et al. 1988a, 1989; McMillin and Pauly 1988). Many authors therefore have tended to neglect the role of free [ADP] as one of the main regulating factors, in favour of other activation mechanisms (Balaban 1990; Balaban and Heineman 1989; Brown 1992; Conley et al. 1997; Connett 1988; Connett and Honig 1989; Heineman and Balaban 1990; Hochachka and Matheson 1992; Hochachka and McLelland 1997; Kantor et al. 1986; Katz et al. 1989; McMillin and Pauly 1988). These other potential regulatory mechanism have generally been believed to depend on Ca^{2+} activation of NAD^+ dependent dehydrogenases (Territo et al. 2000) and of other mitochondrial key enzymes such as PDH (Hansford and Zorov 1998). The rise of Ca^{2+} caused by muscle contraction has therefore been assumed to enhance the up-regulation of OxP (Territo et al. 2000). Finally, some authors have proposed the inclusion of known potentials – the $\Delta G_{ATP,cyt}$ and the Δp – in the regulation scheme (Barstow et al. 1994; Fontaine et al. 1997).

This paper is restricted to a basic quantitative analysis of the relationship of the cytosolic phosphorylation state to the activity of OxP and glycolysis. It is the aim of this paper to demonstrate that the main control of the rephosphorylating processes in the cells can take place at this level, so that all contradictions discussed above regarding the regulation mechanism of OxP can be resolved. It is also intended to demonstrate that mathematical models derived from the above analysis can be used as tools to simulate the complex dynamic behaviour of metabolic reactions such as OxP and glycolysis, thus contributing to the development of a detailed, consistent, theory of the functions involved.

Basic aspects of a mathematical description of the feedback control of OxP and glycolysis by the phosphorylation state of the CHEP system

The feedback control of glycolysis and OxP requires that the phosphorylation state of the CHEP system is tightly coupled to the rate of glycolysis and OxP, so that a certain degree of the phosphorylation deficit activates OxP and glycolysis, to compensate for an increased rate of dephosphorylation, at rest or during exercise. Feedback control systems of this type are dynamic systems which exhibit two stages:

1. A steady state which is achieved when the *rate of ATP consumption* is equal to the *rate of ATP production*. At a metabolic steady state the CHEP system is at equilibrium; the metabolic rates and the main parameters of the internal environment are constant.
2. Transient states caused by sudden changes of the ATP consumption rates. This may lead either to a new steady state, or to a stage of a non-steady state which can be maintained only for a limited time and within certain limits of the deviation of the inner physico-chemical environment.

Feedback control systems describing the dynamics of the metabolic reactions at the cellular level cannot be established and described without the analysis of the time behaviour of the main parameters of the system (Funk et al. 1990; Mader and Heck 1996; Mader 1998; Meyer 1988). The mathematical description must also include a sufficient set of parameters and equations which determines its behaviour. Then the translation to a computer model allows the comparison of the experimental data generated by the simulation of the system's dynamic to the measured parameter of the real system as obtained by a given experimental procedure. The mathematical description of the elements of the metabolic control systems must be based on a sufficient set of equations governing the parameters of the system and

determining its behaviour. This includes the calculation of:

1. The equilibrium constants of the several reactions among the components of the CHEP system, including the calculation of $\Delta G_{ATP,cyt}$ (kilojoules per mole).
2. The steady state activity characteristics of glycolysis and of OxP. These will be described as functions of the phosphorylation state of the CHEP system, the known activators and the equivalent of $\Delta p'$ (kilojoules per mole). This will be expressed in terms of $\Delta G_{ox,ap}$ (kilojoules per mole) which results from the inner mitochondrial ATP formation by the F_0F_1-ATPase complex and the ATP-ADP-transfer by the ATP^{-4}/ADP^{-3}-translocase. An excellent explanation of these functions is given in Ferguson (2000)
3. The influence of some main parameters of the inner chemical environment of the cell on the chemical equilibrium of the CHEP system and on the activity of OxP and glycolysis.

On these bases, a consistent theoretical description of the main regulation of OxP and glycolysis will be developed, leading to the development of mathematical models of differing accuracies. These will be shown to be essential for an extended quantitative recalculation of the steady state and of the dynamic behaviour of the main parameters of this system, and to be related to all possible experimental situations. This will be feasible only by using differential equations for the calculation of the parameter of the system as a function of time and "functional load" or the disturbances of the system (Mader and Heck 1986, 1996).

Calculation of the equilibrium between PCr and adenosine phosphates

The equilibrium of the cytosolic high energy phosphate system results from the CK reaction:

A. $[ATP]+[Cr]<=====>[ADP]+[PCr]+[H^+]$
including the adenylate kinase reaction:
B. $2[ADP]<=====>[ATP]+[AMP]$
However, reaction (A) is not a real reaction. According to Golding et al. (1995) and others (McGilvery and Murray 1974) the real reactions which are summarized under (A) consist of a set of about 12 reactions including free $[P]_i$, H^+ and Mg^{2+} ions. In contrast to the common interpretation of reaction (A), it can be assumed that [Cr] functions as a template for phosphate binding and the CK reaction can be rewritten as a mirror reaction where the free cytosolic $[P]_i$ replaces [Cr]:
C. $[ATP]+[P]_i<=====>[ADP]+[PCr]+[H^+]$

This takes into account the fact that, under conditions at rest, the content of free [Cr] can vary between 5 and 15 $mmol \cdot kg^{-1}$ wet muscle tissue (Arnold et al. 1984; Conley et al. 1997) but free cytosolic $[P]_i$ is kept at a relative low concentration of about 2 to 4 $mmol \cdot kg^{-1}$ in normal skeletal muscle (Arnold et al. 1984; Barstow et al. 1994; Conley et al. 1997; Connett and Honig 1989; Kushmerick 1987; Kushmerick et al. 1992; Nicholls and Ferguson 1997; Nioka et al. 1992; Taylor et al. 1986; Thompson et al. 1995; Williamson 1979; Wilson 1994). This applies also to muscles with a high oxidative capacity, such as the heart (Balaban 1990; Heineman and Balaban 1990; Kantor et al. 1986; Katz et al. 1988a, 1989; Lewandowski et al. 1987). This indicates that the ATP-PCr equilibrium in vivo is determined by $\Delta G_{ATP,cyt}$ of –58 to –65 $kJ \cdot mol^{-1}$ calculated by Eq. 4 which rules the $[PCr]:[P]_i$ ratio independently of the excess of [Cr]. Therefore, the free energy of the CHEP system $\Delta G_{ATP,cyt}$ is calculated using $[P]_i$ rather then [Cr]; it could be rewritten also as a function of the ratio $[PCr]:[P]_i$ if the limited amount of free cytosolic $[P]_i$ under conditions of rest is taken into account (Barstow et al. 1994). Without this precaution, there is a theoretical inconsistency between the calculation of free [ADP] and $\Delta G_{ATP,cyt}$ on the one hand and the free cytosolic $[P]_i$ and [Cr] on the other. This inconsistency might be one of the causes limiting the understanding of the experimentally known facts regarding the regulation of OxP. Regardless of the excess of [Cr], the free cytosolic $[P]_i$ under conditions of rest is kept within the range, determined by $\Delta G_{ATP,cyt}$, of about –58 to –65 $kJ \cdot mol^{-1}$ as calculated using Eq. 4 (Arnold et al. 1984; Balaban 1990; Barstow et al. 1994; Brown 1992; Heineman and Balaban 1990; Kantor et al. 1986; Kushmerick 1987; Kushmerick et al. 1992; Nicholls and Ferguson 1997; Nioka et al. 1992; Taylor et al. 1986; Thompson et al. 1995; Williamson 1979; Wilson 1994). Since free Mg^{2+} concentration does not influence the CK-equilibrium much, provided it is 1.0 $mmol \cdot l^{-1}$ or more (Golding et al. 1995; Veech et al. 1979), its influence will not be taken into account.

The chemical equilibrium between the components of the CHEP-system is established within a few milliseconds, so, a change of the [ATP]:[ADP] ratio, brought about by dephosphorylation or rephosphorylation processes, leads to an immediately re-established ATP-PCR equilibrium, as indicated by the saturation transfer measurement between [ATP]:[ADP] and $[PCr]:[P]_i$ on living muscle using ^{31}P-NMR (LeRumeur et al. 1997). Thus, it can be assumed that under all conditions in living cells, the CHEP system is near to a simple chemical equilibrium (Arnold et al. 1984; Barstow et al. 1994; Kushmerick 1987; McGilvery and Murray 1974; Taylor et al. 1986; Thompson et al. 1995; Wieseman and Kushmerick 1997).

The equilibrium between $[PCr]:[P]_i$ and the adenosine phosphates ([ATP], [ADP] and [AMP]) including the influence of $[H^+]$ can be calculated at different levels of accuracy (Golding et al. 1995; McGilvery and Murray 1974). The assumption that reaction (C) is the mirror reaction of (A), coupled with reaction (B) provides the simplest algebraic solution in the calculation of the

ATP-PCr equilibrium during dynamic changes in the concentration of the CHEP system (see Eqs. 6, 7 and 8). According to reaction (C) [ATP] and [PCr] at equilibrium are described by:

$$\mathbf{1)}\ [\mathbf{ATP}]/[\mathbf{ADP}] = \mathbf{M_1} \times [\mathbf{PCr}]/[\mathbf{P}]_i \quad (1)$$

with M_1 equal to the apparent equilibrium constant.

Since the ATP-PCr equilibrium depends on pH_m, the apparent CK equilibrium constant M_1 is given by the product $M_2 \times [H^+]$ [$M_2 = 1.66 \times 10^9 \cdot mol^{-1}$ (Veech et al. 1979)]. Rearranging Eq. 1 the level of free [ADP] can be calculated as:

$$\mathbf{2)}\ [\mathbf{ADP}] = [\mathbf{ATP}] \times [\mathbf{P}]_i/(\mathbf{M_2} \times [\mathbf{H^+}] \times [\mathbf{PCr}]). \quad (2)$$

Free [AMP] can be calculated from [ADP] using the following equation (see reaction B):

$$\mathbf{3)}\ [\mathbf{ATP}] \times [\mathbf{AMP}] = \mathbf{M_3} \times [\mathbf{ADP}]^\mathbf{2} \quad (3)$$

where M_3 is the equilibrium constant (from approximately 0.85–1.05) (Krause and Wegener 1996; Newsholme and Start 1973). According to Eq. 3 [AMP] is related to $[ADP]^2$; therefore the product [AMP] × [ADP] is approximately equivalent to $[ADP]^3$ (Mader et al. 1983; Mader and Heck 1986, 1996).

The free energy of the CHEP system ($\Delta G_{ATP,cyt}$) is determined by the quotient of [ATP]/([ADP] × [P_i]), which represents the state of phosphorylation and can be calculated by:

$$\mathbf{4)}\ \Delta G_{\mathbf{ATP,cyt}}(\mathbf{kJ \cdot mol^{-1}}) = \Delta G_\mathbf{0} - \mathbf{R} \times \mathrm{T} \times \mathbf{ln}([\mathbf{ATP}]/([\mathbf{ADP}] \times [\mathbf{P}]_i)) \quad (4)$$

with $\Delta G_0 = -30.6\ kJ \cdot mol^{-1}$.

If it is assumed that S[A] = [ATP] + [ADP] + [AMP] and if S[C] = [PCr] + $[P]_i$ (because free [Cr] is normally present in excess over $[P]_i$) this system represents the amount of substrate available for energy storage. If, as a first approach, S[A] and S[C] are assumed constant, the phosphorylation deficit of the CHEP system can be expressed either by the difference S[A]–[ATP] or by the difference S[C]–[PCr]. This allows the construction of an algebraic solution to calculate free [ADP] as a function of the difference S[C]–[PCr], including the influence of $[H^+]$ on the [ATP]-[PCr] equilibrium, where S[C] represents the sum of the active compounds [PCr] + $[P]_i$ related to true conditions of rest.

Furthermore, since the equilibrium assumption is also valid for $\Delta G_{ATP,cyt}$, this allows a direct calculation of $\Delta G_{ATP,cyt}$ from the quotient [PCr]/(S[C]–[PCr]). Substitution of [ADP], as given by the right side of Eq. 2, in Eq. 4 the range of $\Delta G_{ATP,cyt}$ of the CHEP system can be obtained from the [PCr]/$[P]_i$ quotient, including the influence of $[H^+]$, if it is assumed that $[P]_i$ is the chemical active factor. Introducing the above definitions ([ATP] + [ADP] + [AMP] = S[A] and [PCr] + $[P]_i$ = S[C]) then the phosphorylation state of the CHEP system is indicated by the common term S[C]–[PCr] of the following Eqs. 5, 6, 7 and 8 (Mader and Heck 1996):

$$\mathbf{5)}\ \Delta G_{\mathbf{ATP,cyt}}(\mathbf{kJ \cdot mol^{-1}}) = \Delta G_\mathbf{0} - \mathbf{R} \times \mathrm{T} \times \mathbf{ln}\left\{\mathbf{M_2} \times [\mathbf{H^+}] \times [\mathbf{PCr}]/(\mathbf{S[C]} - [\mathbf{PCr}])^\mathbf{2}\right\} \quad (5)$$

$$\mathbf{6)}\ [\mathbf{ADP}] = \mathbf{S[A]}/\{\{(\mathbf{M_3} \times (\mathbf{S[C]} - [\mathbf{PCr}])/\mathbf{M_2} \times [\mathbf{H^+}] \times [\mathbf{PCr}]\} + \{\mathbf{M_2} \times [\mathbf{H^+}] \times [\mathbf{PCr}]/(\mathbf{S[C]} - [\mathbf{PCr}])\} + \mathbf{1}\} \quad (6)$$

$$\mathbf{7)}\ [\mathbf{ATP}] = \mathbf{M_2} \times [\mathbf{H^+}] \times [\mathbf{PCr}] \times [\mathbf{ADP}]/(\mathbf{S[C]} - [\mathbf{PCr}]) \quad (7)$$

including the calculation of free AMP which is:

$$\mathbf{8)}\ [\mathbf{AMP}] = \mathbf{S[A]} - [\mathbf{ATP}] - [\mathbf{ADP}]. \quad (8)$$

The use of Eqs. 5 , 6, 7 and 8 for calculating the equilibrium of the high energy phosphates in the cytosol has the advantages that the phosphorylation deficit (= S[C]–[PCr]) and $\Delta G_{ATP,cyt}$ of the CHEP system are calculated on a unified basis and the relationship between $[P]_i$ and [PCr] can be determined by ^{31}P-NMR-spectroscopy with the possibility of calculating free cytosolic [ADP] as well as $\Delta G_{ATP,cyt}$ using the same set of experimentally measurable values.

The interplay of the different variables of the system as predicted by Eqs. 5, 6, 7 and 8 is displayed in Figs. 1 and 2 as a function of the sum $[P]_i$ + [ADP] + [AMP]. The above description of the equilibrium conditions of the components of the CHEP system, at the simplest possible level, also provides the basis for the calculation of the activity of glycolysis and oxidative phosphorylation as a function of the phosphorylation state of the CHEP system. This problem will be tackled in the next section.

Calculation of the steady-state activation of OxP

If the oxygen supply at the tissue level is sufficient, the rate of OxP (and as a consequence the rate of $\dot{V}O_2$ by mitochondria) is to a large extent determined by free cytosolic [ADP] as substrate. According to Chance and Williams (1955) the in vitro ratio $v_{vss}/v_{max} = 0.5$ is achieved at about 0.035 $mmol \cdot l^{-1}$ free [ADP]. The *steady-state* activity of OxP expressed as rate of $\dot{V}O_{2,ss}$ per kilogram muscle may be calculated using the Hill equation (mathematical description of an MM-kinetic having an exponent greater than 1: for details see Newsholme and Start 1973) as a function of free [ADP] and $\dot{V}O_{2max}$ (Mader et al. 1983; Mader and Heck 1986, 1996) from:

$$9)\ \dot{V}O_{2,ss} = \dot{V}O_{2,max}/(1 + ks'_1/[ADP]^{nox}) \quad (9)$$

The coefficient ks'_1 is the 50% activation rate constant related to the exponent *nox*. This exponent must be greater than 1.0, since using the MM-kinetic with an exponent *nox* = 1.0 it is mathematically impossible to calculate an appropriate activation of $\dot{V}O_2$ as an exclusive function of [ADP]. A reasonable value for the exponent *nox* can be assumed to be in the range of 1.4 or higher, to

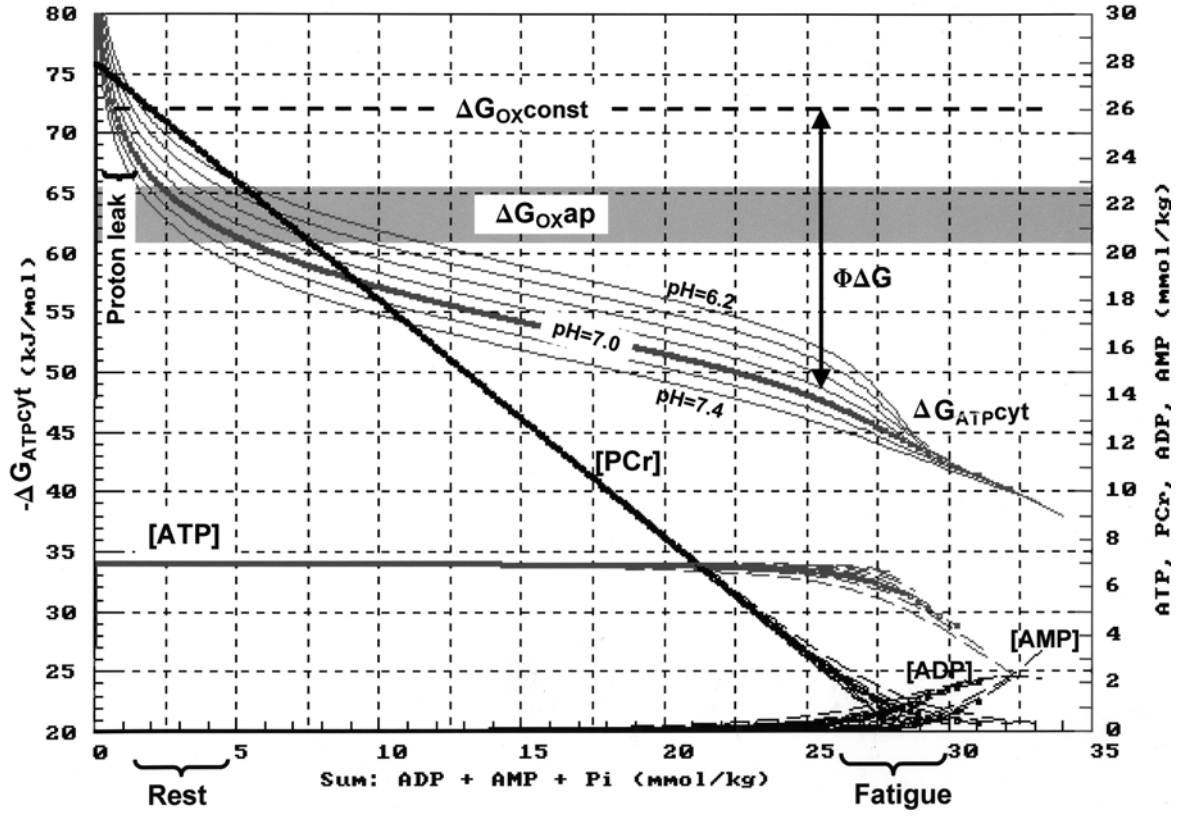

Fig. 1 Phosphorylation relationships according to McGilvery and Murray (1974), on a linear scale. The free energy $\Delta G_{ATP,cyt}$ (kJ·mol^{-1}) is calculated using Eqs. 4 or 5, for S[A] = 7.0 mmol·kg^{-1}, S[C] = 28 mmol·kg^{-1} muscle, CK equilibrium constant $M_1 = 1.66 \cdot 10^9 \cdot mol^{-1}$ and $M_3 = 1.05 \cdot mol^{-1}$ (McMillin and Pauly 1988; Taylor et al. 1986), for intracellular *pH* values from 6.2 to 7.4 in steps of 0.2. The state of phosphorylation for a well-oxygenated muscle at rest (pH = 7.0) is in the range indicated by *Rest*. Fatigue is related to pH = 6.4 and [PCr] close to 0 and is indicated by *Fatigue*. In conditions of rest the free energy ΔG_{ATP}cyt of the CHEP-system is close to $\Delta G_{ox,ap}$ (–60 to –65 kJ·mol^{-1}) generated by the apparent Δp. The constant $\Delta G_{OX,const}$ = –72.5 kJ·mol^{-1} is related to the rate of OxP at rest, caused by the *proton leak*. As indicated by the *arrow*, with increasing dephosphorylation of the CHEP system, the potential difference $\phi\Delta G$ between ΔG_{OX}const and ΔG_{ATP}cyt increases linearly. For more information see text and list of abbreviations

establish a (slightly) sigmoidal activation characteristic (Mader and Heck 1996), (see Fig. 3). Expressed in terms of free [ADP] ks'_1 is assumed to be in the range of 0.035 mmol·l^{-1} (Chance and Williams 1955; Nioka et al. 1992).

The values (ks'_1 = 0.035 mmol·l^{-1} and nox = 1.4) will be used, even if recent experiments favour a Hill equation (Newsholme and Start 1973) with Km(0.5) = 0.048 mmol·l^{-1} free ADP and an exponent close to 2.0 (Cieslar and Dobson 2000). Indeed, many experimental results are consistent with a 50% activity constants Km(0.5) related to free [ADP] in the range between 0.020 and 0.050 mmol·l^{-1} (Barstow et al. 1994; Kushmerick et al. 1992; Nioka et al. 1992; Thompson et al. 1995). It should also be noted that $\dot{V}O_{2max}$ is related to the mitochondria volume of the muscle cell and the P/O-quotient in living mitochondria is approximately constant and independent from the rate of OxP; therefore the rate of OxP is a linear function of $\dot{V}O_2$, as pointed out in detail later (Nicholls and Ferguson 1997).

The functional origin of the exponent *nox > 1.0* using the half maximal rate constant ks'_1 approximating 0.035 mmol·l^{-1} free ADP needs a thorough explanation. The respiratory chain generates a pmf (Δp approximately –0.22 V) across the inner mitochondrial membrane which is approximately equivalent to a Δp′ of –21.7 kJ·mol^{-1} (Nicholls and Ferguson 1997) (see. Fig. 4). This leads to a value of $\Delta G_{ATP,cyt}$ in the range between –58 and –65.0 kJ·mol^{-1} under conditions of rest, generated in two steps. The first step consists in the F_0F_1-ATPase complex harvesting the energy of three protons to build one ATP molecule in the matrix space: thus the mitochondrial F_0F_1-ATPase complex acts as a *potential converter* of Δp′ in its equivalent the *inner mitochondrial phosphorylation potential* (for more details see Ferguson 2000). This can be calculated in terms of $\Delta G_{ATP,mit}$, according to Ferguson (2000) and Williamson (1979) using:

$$\mathbf{10)}\ \Delta G_{ATP,mit}(kJ^{-1}) \tilde{} x \times \Delta p'(kJ^{-1}) \qquad (10)$$

If $x = 3$ is a fixed number of transferred protons $\Delta G_{ATP,mit}$ ought to be about $3 \times -22 = -66$ kJ·mol^{-1}. However, because of a less than optimal efficiency, the resulting $\Delta G_{ATP,mit}$ is about –55 kJ·mol^{-1} (Fig. 4). The energy of another proton is then added to $\Delta G_{ATP,mit}$ at the level of the ATP^{-4}/ADP^{-3} translocase (Ferguson

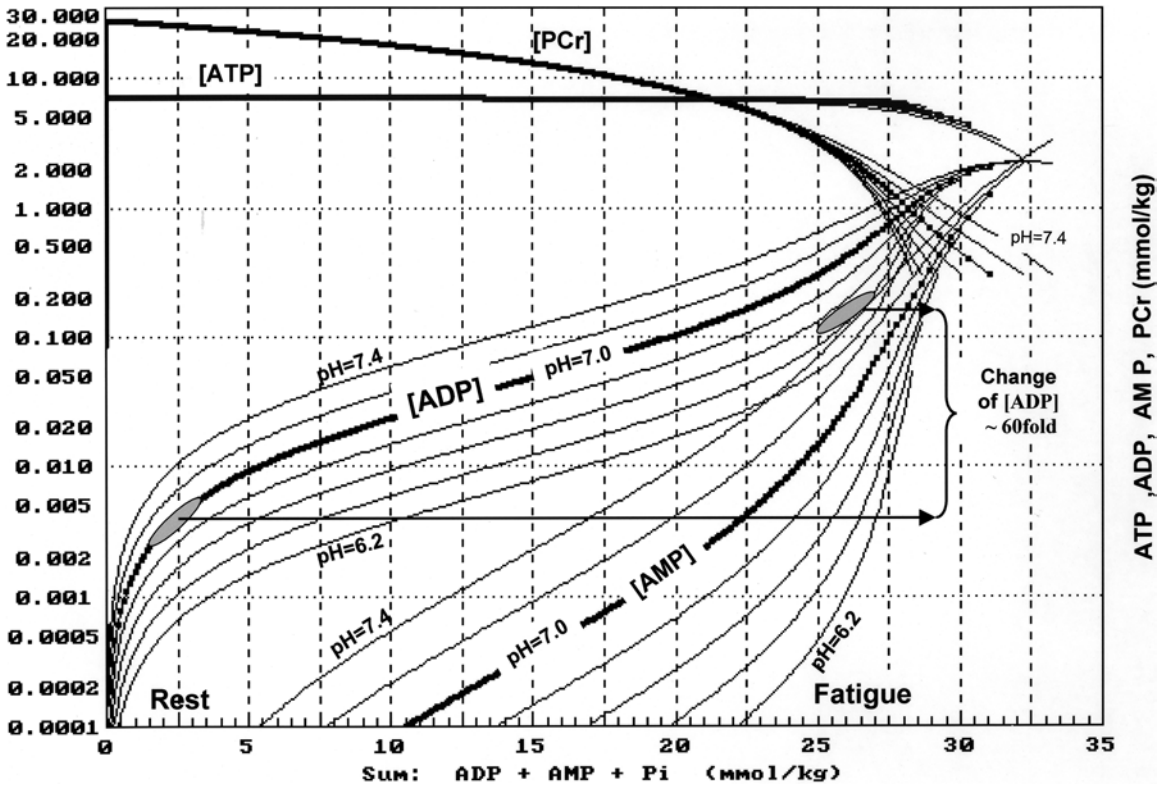

Fig. 2 Phosphorylation relationships on a semi logarithmic scale. For every constant *pH*, an *iso-pH-equilibrium curve* for *[ADP]*, *[AMP]*, *[ATP]* and *[PCr]* as the function of the sum of [ADP]+[AMP]+[P]$_i$ is calculated according to Eqs. 6, 7 and 8. Equilibrium constants and concentrations as in Fig. 1. It can be seen that free [ADP] at rest is of the order of 0.004 mmol·kg^{-1}, close to the values calculated from ^{31}P-NMR-spectroscopy data, to attain values at fatigue of about 0.2 mmol·kg^{-1} at a pH of about 6.4. From rest to fatigue free cytosolic [ADP] increases by a factor of 60. For abbreviations see list

2000). The resulting driving force $\Delta G_{ox,ap}$ at the inner mitochondrial membrane is described by:

$$\mathbf{11)}\ \Delta G_{ox,ap}(kJ^{-1}) \curlywedge (x+1) \times \Delta \mathbf{p}'(kJ \cdot mol^{-1}) \qquad (11)$$

Again, because of the less than optimal efficiency the resulting $\Delta G_{ox,ap}$ amounts to about –72.5 kJ·mol^{-1} or less (Fig. 4).

The second step consists in a fall of $\Delta G_{ox,ap}$ to the actual value within the cytosol. The resulting potential difference $\Phi\Delta G$ (approximately equal to $\Delta G_{ox,ap} - \Delta G_{ATP,cyt}$) is the driving force which is necessary to sustain the flow of ATP from inside the mitochondrian to the cytosol. Since the flow rate of ATP is also proportional to the difference $\Delta G_{ox,ap} - \Delta G_{ATP,cyt}$ it also follows that $\Phi\Delta G$ is approximately linearly related with the difference in the rate of OxP between rest and $\dot{V}O_{2max}$. Making this assumption the effect of an increase of free cytosolic [ADP] itself can be described by the MM-kinetics, associated with a second driving force $\Phi\Delta G_{ADP}$ given by the difference:

$$\mathbf{12)}\ \phi\Delta G_{ADP} = \mathbf{ks_{1DG}} \times (\Delta G_{\mathbf{OX},ap} - \Delta G_{\mathbf{ATP},cyt}) \qquad (12)$$

between the inner mitochondrial membrane and the cytosol. Using this relationship Eq. 9 can be rewritten under these restrictions as:

$$\mathbf{13)}\ \dot{V}O_{2,ss} = \dot{V}O_{2,max}/\{\mathbf{1} + \mathbf{ks_1}/([\mathbf{ADP}] \times \phi\Delta G_{ADP})\} \qquad (13)$$

This is consistent with the known structure of the generation of mitochondrial ATP, including two independent but tightly coupled processes: firstly, the generation of the Δp which in turn generates $\Delta G_{ox,mit}$ by the formation of ATP inside the mitochondria and, secondly, the delivery of ATP from inside mitochondria to the cytosol.

There are many facts that support this assumption:

1. Mitochondria in vitro exhibit only a slight decrease of the *apparent* Δp with an increase of the rate of $\dot{V}O_2$ (Nicholls and Ferguson 1997) which is assumed to be reflected in $\Delta G_{ox,ap}$ remaining also approximately constant. That means that the rate of OxP increases linearly in relation to the difference $\Delta G_{ox,ap}$–$\Delta G_{ATP,cyt}$ between the rate at rest and the maximal rate (see Figs. 1, 3 and 4).
2. In resting well oxygenated muscles with a low rate of OxP the difference between $\Delta G_{ox,ap}$ and $\Delta G_{ATP,cyt}$ comes close to 0 and the system comes close to equilibrium (see Figs. 1, 3 and 4).

In Eq. 13 an equivalence between the change of [ADP] and the change of $\Delta G_{ATP,cyt}$ is proposed. Calculated using Eq. 5 and 6 at $pH_m = 7.0$ a tenfold increase of free [ADP] from 0.01 to 0.1 mmol·l^{-1} would be associated with a decrease of $\Delta G_{ATP,cyt}$ of about 8 kJ·mol^{-1} towards 0. But this would mean also that an increase of

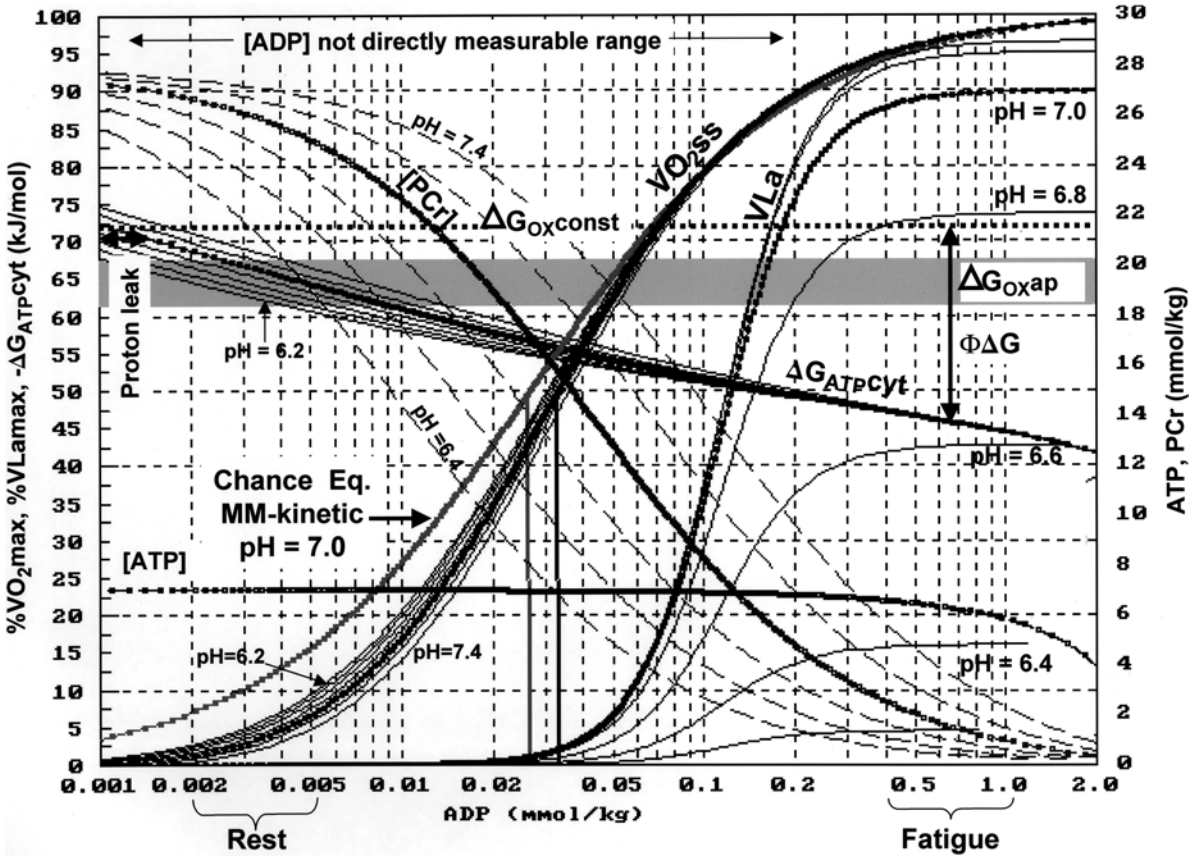

Fig. 3 Steady-state activities of oxidative phosphorylation (OxP being approximately equivalent to $\dot{V}O_{2,ss}$) and glycolysis (approximately equivalent to VLa), expressed as percentages of $\dot{V}O_{2max}$ and VLa_{max}, as functions of log free cytosolic *[ADP]*. The *thick lines* refer to values at pH = 7.0. The *MM-kinetic* having a 50% activity constant Km(0.5) of 0.027 mmol·l^{-1} free [ADP] is indicated by an *arrow*. The activation *curve* according to Eq. 13 is based on a 50% activity constant ks_1 of 0.035 mmol·l^{-1} free [ADP] at pH = 7.0. The $\dot{V}O_{2,ss}$ *curve* which represents the rate of OxP and the *curve* of *[PCr]* are mirror images displaying a linear relationship within the physiological range of OxP activity. The cytosolic [H^+] contribute to the difference $\Delta G_{OX}const$–$\Delta G_{ATP}cyt$ during rest and moderate activation of the respiratory chain. Therefore, different *iso-pH* activation curves of OxP are calculated. Free energy ΔG_{ATP}cyt decreases linearly with increasing log free [ADP]. Activation of glycolysis is calculated according to Eq. 16. For abbreviations see list

$\Phi\Delta G_{ADP}$ is equivalent to an increase of free [ADP] as calculated in Eq. 12. Therefore, [ADP] would increase with the 2nd power of the difference $\Delta G_{ox,ap}$–$\Delta G_{ATP,cyt}$, thus explaining the experimentally observed exponent *nox* being more than 1.0. The conclusion is that the rate of OxP is driven not only by its substrate ADP but also by a potential difference of free energy along the chain of $\Delta G_{ox,ap}$ down to $\Delta G_{ATP,cyt}$, which drives:

1. ATP formation inside the mitochondria
2. The ATP-ADP exchange from mitochondria to the cytosol and performs
3. The down-regulation of free [ADP] at the cytosolic side.

To avoid calculations of the changes of the *apparent* $\Delta p'$ and $\Delta G_{ox,ap}$ as a function of other possible influencing factors without a clear mathematical basis in CS $\Delta G_{ox,ap}$ is replaced by a constant ($\Delta G_{ox,const}$) which remains uninfluenced by the rate of OxP up to $\dot{V}O_{2max}$. It is assumed that $\Delta G_{ox,const}$ is close to a possible equilibrium ($\Delta G_{ox,const} = \Delta G_{ATP,cyt}$) at a very low rate of OxP related to the proton leak. In the CS (see Figs. 5, 6, 7, 8, 9 and 10) $\Delta G_{ox,const}$ is set to –72.5 kJ·mol^{-1}. Under these assumption the coefficient ks_{1DG} of Eq. 12 has values of about $-0.65 \cdot 10^{-4}$ up to $-0.95 \cdot 10^{-4}$·mol^{-1} per 1.0 J·mol^{-1} if ks_1 is 0.035 mmol·l^{-1} free ADP.

Calculation of the steady-state activity of glycolysis

Glycolysis is regulated mainly by the activation of PFK. The PFK is activated by free [ADP], [AMP] and $[P]_i$ and inhibited by a high [ATP], low pH_m and high concentration of citric acid (Krause and Wegener 1996; Newsholme and Start 1973). It should also be noted that the activity of glycolysis is regulated in part also by the level of phosphorylase andPK. The PFK activity depends on the product [ADP] × [AMP] which implies that [AMP] is a factor which amplifies the activation of PFK due to [ADP] (Krause and Wegener 1996; Newsholme and Start 1973). The inhibition of PFK caused by high [ATP] is not removed with the decrease of the phosphorylation state of the CHEP system in the cells because the change of ATP is negligible. The PFK-activity is regulated also by fructose-2,6-bisphosphate, but it seems that this factor keeps PFK active and is there-

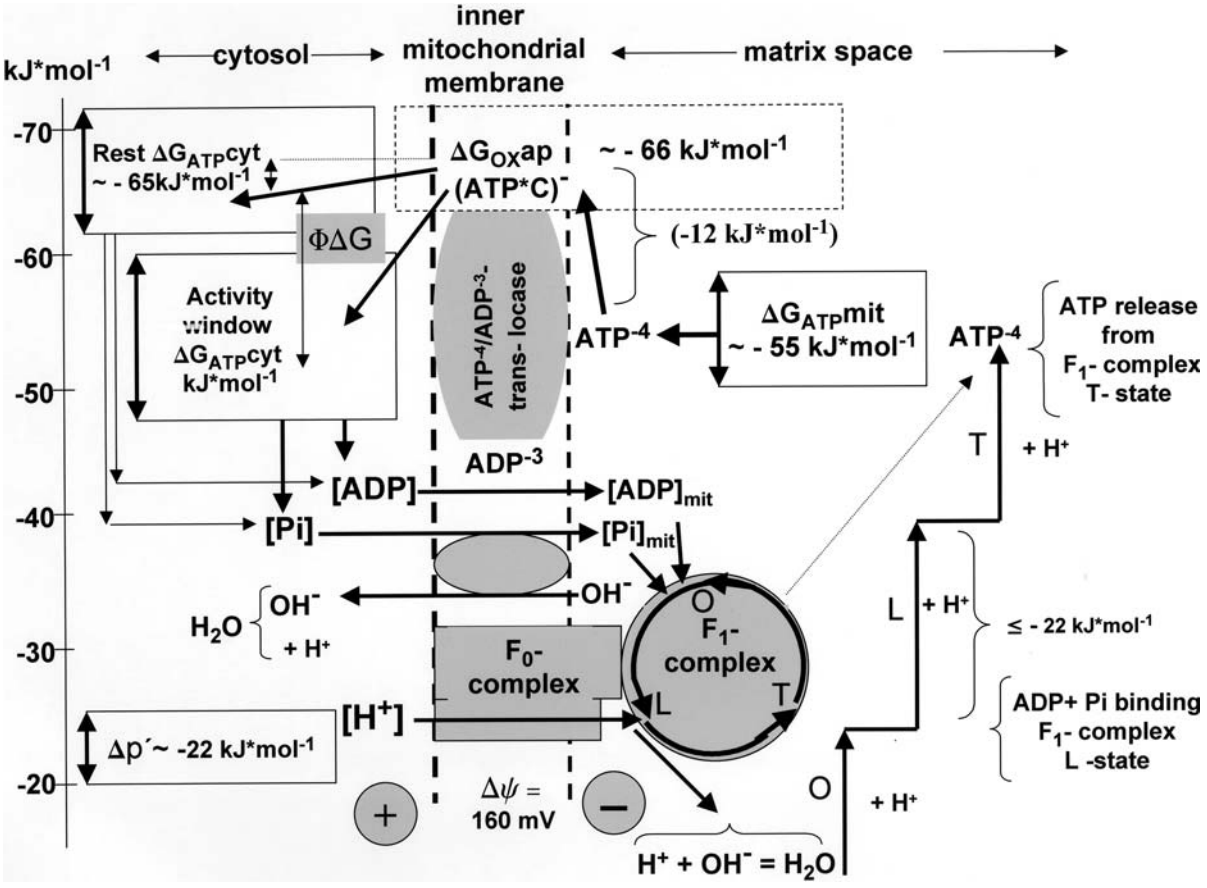

Fig. 4 Diagram of a potential scheme of *ATP*-synthesis at the inside of the inner mitochondrial membrane and of the ATP transfer to the cytosol via ATP/ADP translocase along the potential differences generated from $\Delta G_{OX}ap$ of about –66 kJ·mol^{-1} down to $\Delta G_{ATP}cyt$ of about –62 kJ·mol^{-1} at rest. The $\Delta G_{ATP}mit$ is assumed to be –55 kJ·mol^{-1}, built up by the F_0F_1-complex harvesting the energy of three protons by changing the conformation of the β subunit of the F_0F_1-ATPase from open (*O*) to low (*L*) to tense (*T*) state. According to Klingenberg (1980) the ATP^{-4}/ADP^{-3} translocase forms an ATP-carrier complex by adding about –12 kJ·mol^{-1} to ΔG_{ATP}mit powered by the transmembrane potential $\Delta\psi$ of about –160 mV. This results in a 5:1 preference of ATP efflux from the matrix space compared to the *ADP* uptake, contributing to the down-regulation of free cytosolic [ADP] during rest (Klingenberg 1980). The ATP-carrier complex is assumed to represents ΔG_{ox}ap at the cytosolic side of the inner mitochondrial membrane. With an increasing rate of ATP-consumption by the contraction process ΔG_{ATP}cyt decreases, whereas ΔG_{OX}ap remains approximately constant. Free cytosolic [ADP] increases together with the difference $\Delta G_{OX,}ap–\Delta G_{ATP}cyt = \phi\Delta G$ (see Eq. 13). For abbreviations see list

fore prone to be regulated, or that it acts to enhance the magnitude of the rate control (Krause and Wegener 1996). Using [ADP] and [AMP] as activating modulators of PFK-activity, the Hill equation (Newsholme and Start 1973):

$$\textbf{14)}\ v_{la,ss} = v_{la,max}/\{\mathbf{1} + \mathbf{ks_2}/([\mathbf{ADP}] \times [\mathbf{AMP}])\} \qquad (14)$$

describes the rate of lactate (pyruvate) formation at "steady state" in the case of a pH_m above 7.4. The time constant of this reaction is in the order of a few milliseconds. Therefore every change of the rate of glycolysis is essentially at steady state (Mader et al. 1983; Mader and Heck 1986, 1996). The coefficient $ks_2 = 0.00035$ is the apparent 50% activation rate constant of glycolysis due to PFK activation, which is achieved for a free [ADP] of 0.15 mmol·l^{-1}. It should also be pointed out that the $v_{la,max}$ expressed in terms of millimoles per second per kilogram is a function of the concentration of glycolytic enzymes.

The maximal PFK activity is achieved at a pH_m higher than 7.2 (Danforth 1965). The rate of glycolysis decreases with the fall in pH_m. The in vitro inhibition of PFK by decreasing pH_m shows a sigmoidal shape (Trivedi and Danforth 1966), so that the rate of lactic acid production falls below 10% of its possible maximum at a pH_m of about 6.2 (Danforth 1965; Spriet et al. 1987a). At a normal pH_m of 6.9–7.0, glycolysis can be activated to about 90% of its maximum (Danforth 1965). Many studies have reported an almost complete cessation of glycolysis in vitro and in vivo after maximal repeated contractions under anaerobic conditions at a pH_m of about 6.4 to 6.3 associated with the cessation of contraction (Kent-Braun et al. 1993; Kushmerick 1987; Taylor et al. 1986; Thompson et al. 1995). Similar behaviour has been observed in muscle biopsy specimens from human muscle taken immediately after exhausting exercise (Sahlin et al. 1975; Spriet et al. 1987a, b). As the

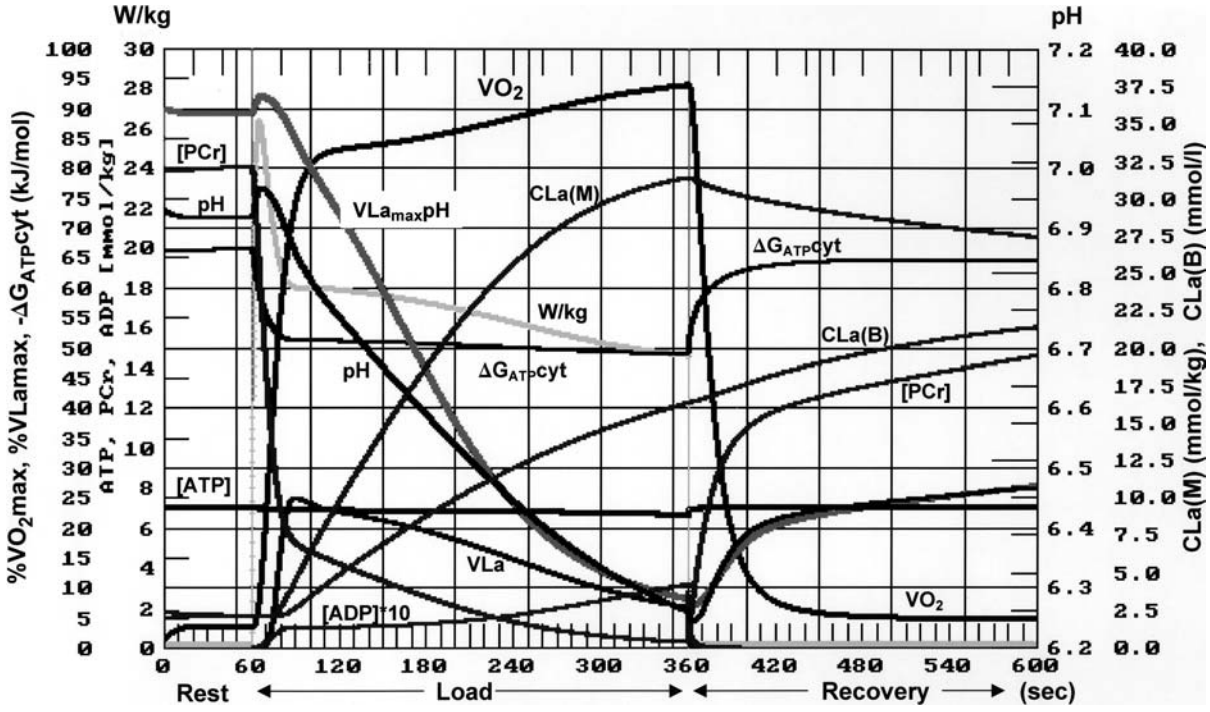

Fig. 5 Computer simulation of a maximal load leading to fatigue as a consequence of PCr-depletion and acidosis caused by lactate accumulation in muscles of low oxidative and medium glycolytic power [$\dot{V}O_{2max} = 158$ ml·min^{-1}·kg^{-1} (about 3.75% Mit Vol, and approximately equal to 4.0 ml O_2·min^{-1}·kg^{-1}), average power output about 16.9 W·kg^{-1}. Additional time constant $\tau\dot{V}O_2 = 9.0$ s, $VLa_{max} = 1.0$ mmol·s^{-1}·kg^{-1}. The transient response of $\dot{V}O_2$, the rate of glycolysis $VLa_{ss}pH$ (= *VLa*), the concentration of lactate in muscle (CLa_M) and blood (CLa_B) are similar to measurements in experiments. The available $VLa_{max,pH}$ is related to the intracellular *pH*. The continuous decrease of $VLa_{ss}pH$ (= VLa) along with the accumulation of lactate is compensated by the slight increase of free *[ADP]*, which activates OxP. The slight but continuous decrease of PCr after the initial fall is compensated in part by the shift of the ATP-PCr equilibrium towards *[ATP]*, which allows a near complete dephosphorylation of *[PCr]* with less influence on ATP-content. The stage of fatigue is reached at the complete breakdown of [PCr] and the occurring decline of the ATP concentration. This occurs when the actual VLa (= $VLa_{ss}pH$) comes close to $VLa_{max}pH$. For abbreviations see list

inhibition of PFK by increasing [H^+] is noncompetitive, the decrease in the function in those enzymes which remains prone to activation, and hence the maximal rate of lactate formation can be calculated as follows (Mader et al. 1983; Mader and Heck 1996):

$$\textbf{15)}\ v_{la,max}\mathbf{pH} = v_{la,max}/(\mathbf{1} + [\mathbf{H}^+]^{\mathbf{3}}/\mathbf{ks_3}) \quad (15)$$

Combining Eqs. 14 and 15:

$$\textbf{16)}\ v_{la,ss}\mathbf{pH} = v_{la,max}/\Big\{(\mathbf{1} + [\mathbf{H}^+]^{\mathbf{3}}/\mathbf{ks_3}) \times [\mathbf{1} + \mathbf{ks_2}/([\mathbf{ADP}] \times [\mathbf{AMP}])]\Big\} \quad (16)$$

where ks_3 is about $10^{-20.2}$.

Thus under conditions of rest the formation of pyruvate or lactate is equal to 0.03 mmol·kg^1·min^{-1} or less if an average $v_{la,max}$) of 1.0 mmol·s^{-1}·kg^{-1} in muscles of mixed red oxidative and white glycolytic fibres is assumed (Spriet et al. 1987a).

A decreasing pH_m contributes to the inactivation of glycolysis by the shift of the ATP-PCr equilibrium to ATP, which decreases [ADP] and [AMP] as was the case for [PCr]. The Eqs. 14, 15 or 16 do not explain the special details of the mechanism of the regulation of PFK activity. They simply provide a basis for a precise calculation of the experimentally observed range of the rate of glycolysis between conditions of rest and maximal activation due to a maximal power output of the contraction process (Mader et al. 1983; Mader and Heck 1986, 1996).

Steady-state characteristic of lactate elimination by combustion

Lactate oxidation in the mitochondria of working muscles depends on $\dot{V}O_2$ and pyruvate (lactate) concentration at the level of PDH (Donovan and Brooks 1983; Katz et al. 1989; Parolin et al. 1999). It should also be noted here that the reaction between lactate and pyruvate is always close to equilibrium. The average amount of pyruvate oxidized per unit O_2 consumed is 0.01475 mmol·ml^{-1} O_2 (Donovan and Brooks 1983; Mader and Heck 1986; Mader 1999). Therefore a pyruvate formation of 0.03 mmol·min^{-1}·kg^{-1} needs 2.0 ml O_2·min^{-1}·kg^{-1} for its combustion. The $\dot{V}O_2$ in the muscles at rest is at about this level or slightly higher. Experimental data show that lactate elimination by mitochondrial combustion $v_{la,ox}$ is a linear function of the current $\dot{V}O_2$ and nonlinearly related to lactate concentration (Donovan and Brooks 1983; Mader and Heck 1986); it can be calculated using the following equation:

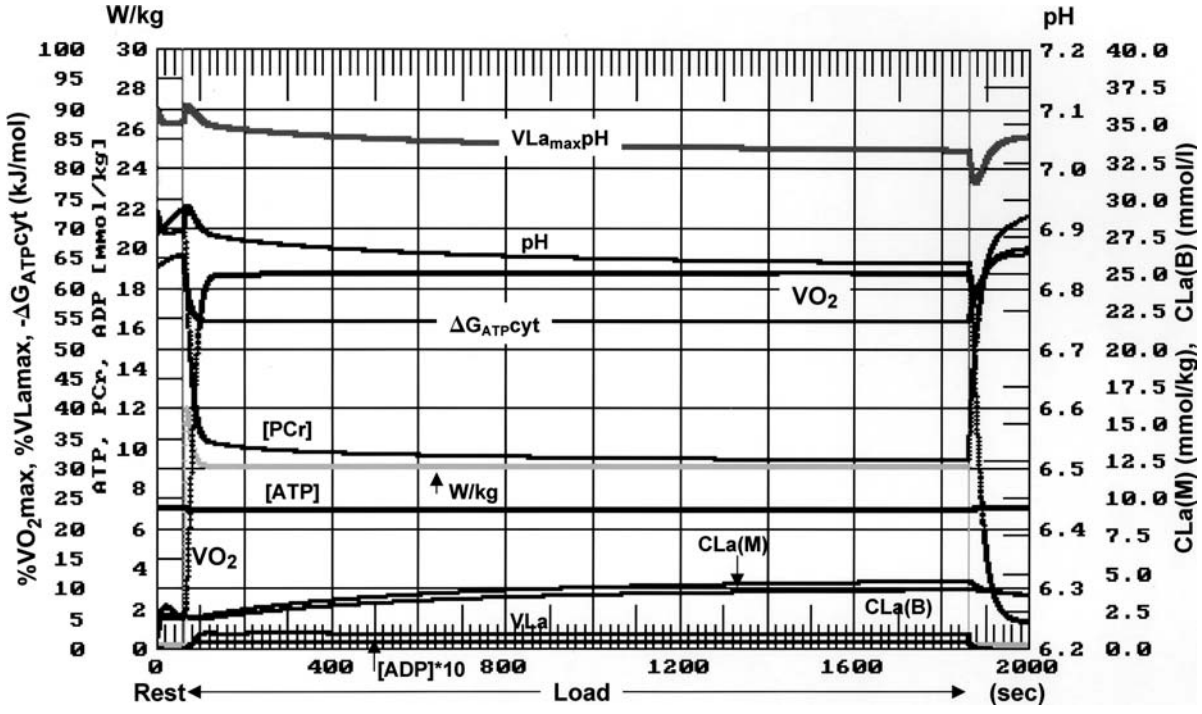

Fig. 6 Computer simulation of a work load corresponding to the anaerobic threshold establishing a maximal oxidative steady state at about 63% of $\dot{V}O_{2max}$. After a small initial rise, *CLa(M)* and *CLa(B)* become constant, amounting to about 4 mmol·kg^{-1}. Average mechanical power is about 9.10 W·kg^{-1}, other data are as in Fig. 5. The contribution of $VLa_{SS}pH$ (=VLa) accounts for about 6% of the total energy demand. More than 95% of the produced pyruvate is oxidized as mitochondrial fuel. For abbreviations see list

$$\mathbf{17)}\ v_{la,ox} = \mathbf{0.021} \times \dot{V}O_{2,a}/(\mathbf{1}+k_{el,ox}/[la^-]^{\mathbf{2}}) \qquad (17)$$

where [la$^-$] is the lactate concentration. The factor 0.021 results from 0.01475/0.75 where 0.75 is the average muscle H_2O space.

The $k_{el,ox}$ is equivalent to [la] of about $\sqrt{2.0} = 1.45$ mmol·l^{-1} lactate and a metabolic RQ of 0.85 (Mader 1999); it reflects the affinity of PDH to pyruvate as the substrate (Mader and Heck 1986; Mader 1999). As can be seen from Eq. 17, lactate oxidation depends strongly on $\dot{V}O_2$ which determines $[la]_{ss}$ at submaximal workload (Mader and Heck 1986; Mader 1999). During recovery from a metabolic acidosis caused by lactate accumulation, about one-third of the eliminated lactate is resynthesized to glycogen which can be – for reasons of simplicity – added to the rate of lactate oxidation.

Feedback control of the rephosphorylating metabolic activity

The phosphorylation state of the CHEP system is given by the sum [GP]=[ATP]+[PCr]. The dynamic change per unit of time can be expressed by d[GP]/dt (millimoles per second per kilogram) as given by the difference between the GP-production rate (i.e. the instantaneous $v_{GP,\dot{V}O2,a}$) and $v_{GP,v,la}$) and the rate of dephosphorylation ($v_{GP,rest} + v_{GP,E}$) both expressed in terms of (millimoles per second per kilogram). Therefore, at any time, the rate of change of the [GP] can be expressed by the following non-linear differential equation: rate of change of [GP] equals rate of resynthesis from respiration plus glycolysis, minus rate of dephosphorylation from resting metabolic rate plus mechanical power output, or,

$$\mathbf{18)}\ \mathbf{d[GP]}/\mathbf{d}t = v_{GP,\dot{V}O2,a} + v_{GP,v,la} - (v_{GP,rest} + v_{GP,E}). \qquad (18)$$

In Eq. 18, $v_{GP,rest}$ is the basic rate of dephosphorylation which is necessary to maintain life whereas $v_{GP,E}$ is set by the energy demand of the contraction process. The $v_{GP,\dot{V}O2,a}$ is the instantaneous rate of OxP including a time delay resulting from adjustment of the oxygen transport to the consumption rate. The rate of change of $\dot{V}O_{2,a}$ can be calculated using the following differential equation:

$$\mathbf{19)}\ \mathbf{d}\dot{V}\mathbf{O_{2,a}}/\mathbf{d}t = \mathbf{k}_{\dot{V}O2} \times (\dot{V}O_{2,ss} - \dot{V}O_{2,a}) \qquad (19)$$

(Mader and Heck 1996) where the term $\dot{V}O_{2,ss}$ is calculated using Eq. 13 and $k_{\dot{V}O2} = 1/\tau_{\dot{V}O2}$ is a *delay rate constant*, which is supposed to be in the range of 4–10 s for the skeletal muscle, leading to an apparent total time constant of 15 up to 35 s in the CS of the rise of $\dot{V}O_2$, approaching a steady state under conditions of a constant load as observed in the whole human body (Barstow et al. 1993; Korecky and Brandejs-Barry 1987; Thompson et al. 1995). In this equation the acceleration of the increase of $\dot{V}O_2$ is proportional to the difference between $\dot{V}O_{2,a}$ and the proposed $\dot{V}O_{2,ss}$ according to the current free [ADP] calculated using Eq. 13. The term

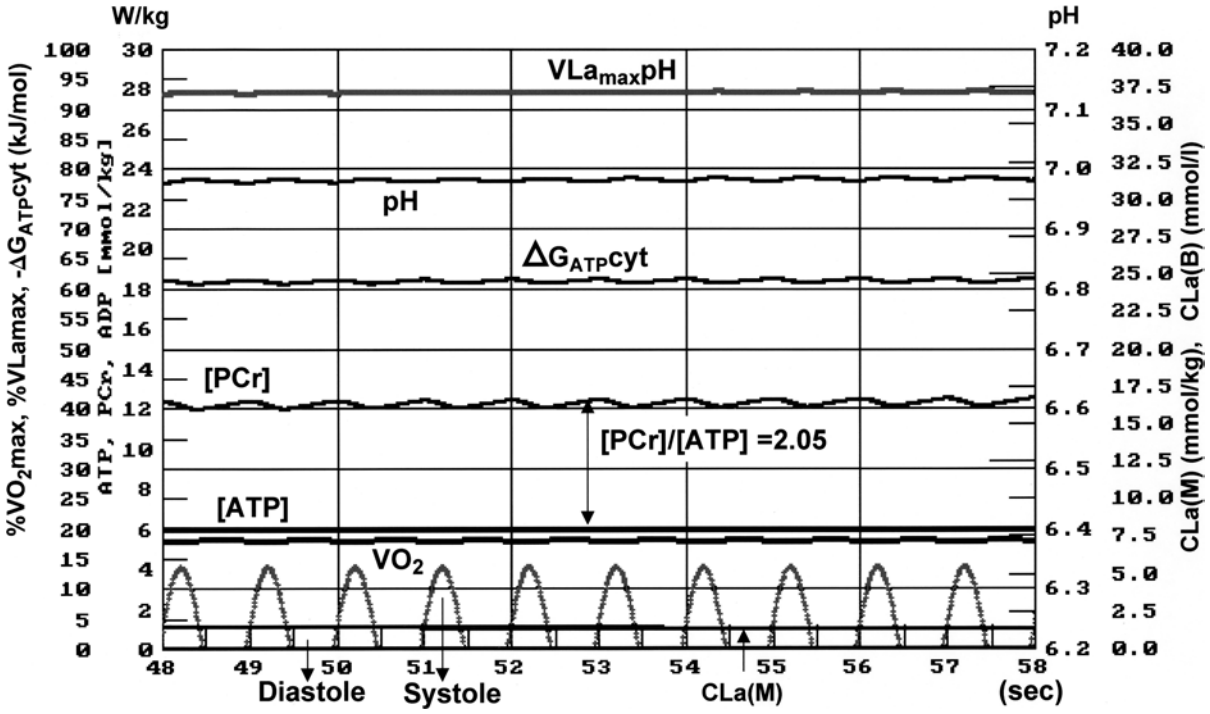

Fig. 7 Computer simulation of a sinus load (1.0 Hz = 60 beats·min^{-1}) on heart muscle having a virtual $\dot{V}O_{2max}$ of about 1,000 ml·min^{-1}·kg^{-1} relating to about 25% V_{mit}. Metabolic power output is about 17% of $\dot{V}O_{2max}$. Mechanical power output is indicated by the *lower peaks*. The Vla and blood lactate concentrations are negligible. The PCr content in conditions of rest when no contraction is occurring is about 14.0 mmol·kg^{-1} assuming a cytosolic space of about 70% of the cell volume. Heart muscle in humans, at the normal frequency at rest of 65 beats·min^{-1} is assumed to consume about 80 ml O_2·min^{-1}·kg^{-1} in the steady state, with a $[PCr] = 12$ mmol·kg^{-1}. This is about one-sixth to one-eighth of the maximal rate of OxP sustainable for more than a few minutes. The consumption of PCr per beat is quite high, the [PCr] content during the contraction cycle being practically constant at about 12.2 mmol·kg^{-1}. The [PCr] [ATP] quotient is 2.05, which is comparable to the real situation in the working heart under the above-mentioned conditions. For abbreviations see list

$\dot{V}O_{2,a}$ (millilitres per second per kilogram) therefore includes the delayed response of $\dot{V}O_2$ at the beginning of exercise, resulting from delayed oxygen transport. The instantaneous $\dot{V}O_{2,a}$ is given by:

$$\mathbf{20)}\ v_{GP,\dot{V}O2,a}(\mathbf{mmol \cdot s^{-1} \cdot kg^{-1}}) = \mathbf{b}_{\dot{V}\mathbf{O2}} \times \dot{V}O_{2,a} \times (\mathbf{ml \cdot s^{-1} \cdot kg^{-1}}) \quad (20)$$

when the coefficient $b_{\dot{V}O2}$ (millimoles per millilitre) is $1/4.3 = 0.233$, because 1.0 mmol ATP or PCr is produced by the consumption of 4.3 ml O_2 (corresponding to a P:O_2 ratio of 5.2). The glycolytic part of the GP-replenishment ($v_{GP,v\ la}$) results from:

$$\mathbf{21)}\ v_{GP,v,la}(\mathbf{mmol \cdot s^{-1} \cdot kg^{-1}}) = \mathbf{b}_{v,la} \times v_{la,ss}\mathbf{pH} \times (\mathbf{mmol \cdot s^{-1} \cdot kg^{-1}}). \quad (21)$$

when $b_{v,la}$ is assumed to be 1.4, since the formation of 1.0 mmol pyruvate or lactate produces from 1.35 to 1.45 mmol ATP (or PCr). The term $v_{la,ss,pH}$ is calculated using Eq. 16. The energy demand of the contraction process, in watts per kilogram muscle mass, must be transformed into a GP consumption rate:

$$\mathbf{22)}\ v_{GP,E}(\mathbf{mmol/s \cdot kg}) = \mathbf{b}_{\mathbf{Pow}}(\mathbf{mmol \cdot kg^{-1} \cdot s^{-1} \cdot W^{-1}}) \times E(\mathbf{W}) \quad (22)$$

The estimation of b_{Pow} depends on the efficiency of mechanical work performed under any given set of conditions for muscle contraction; as such it varies considerably. For the human body during cycle ergometer exercise an increase of between 11.4 and 12.5 ml·min^{-1} O_2·W^{-1} is commonly observed. Thus, assuming that 4.3 ml O_2 are required to produce 1 mmol GP, this corresponds approximately to $12/(4.3 \times 60) = 0.0466$ mmol GP·J^{-1}. The reciprocal of this quantity is the mechanical equivalent of GP splitting, which amounts therefore to 21.5 kJ·mol^{-1}.

The terms ($v_{GP,\dot{V}O2,a} + v_{GPvla}$) in Eqs. 20 and 21 are the given GP-production rates, which depend on the phosphorylation deficit of the CHEP system expressed either by S[A]–[ATP] or by S[C]–[PCr] which are indexes of [ADP] and [AMP]. Therefore substituting Eqs. 20 and 21 into Eq. 18 one obtains:

$$\mathbf{23)}\ \mathbf{d}[\mathbf{GP}]/\mathbf{d}t = \mathbf{b}_{\dot{V}\mathbf{O2}} \times \dot{V}\mathbf{O}_{2,a} + \mathbf{b}_{v,la} \times v_{la,ss}\mathbf{pH} - \mathbf{b}_{\dot{V}\mathbf{O2}} \times \dot{V}O_{2,a,rest} - \mathbf{b}_{\mathbf{Pow}} \times E \quad (23)$$

In this equation, $v_{la,ss,pH}$ is the instantaneous rate of glycolysis, calculated using Eq. 16 as a function of the current concentrations of the activating factors ([ADP]

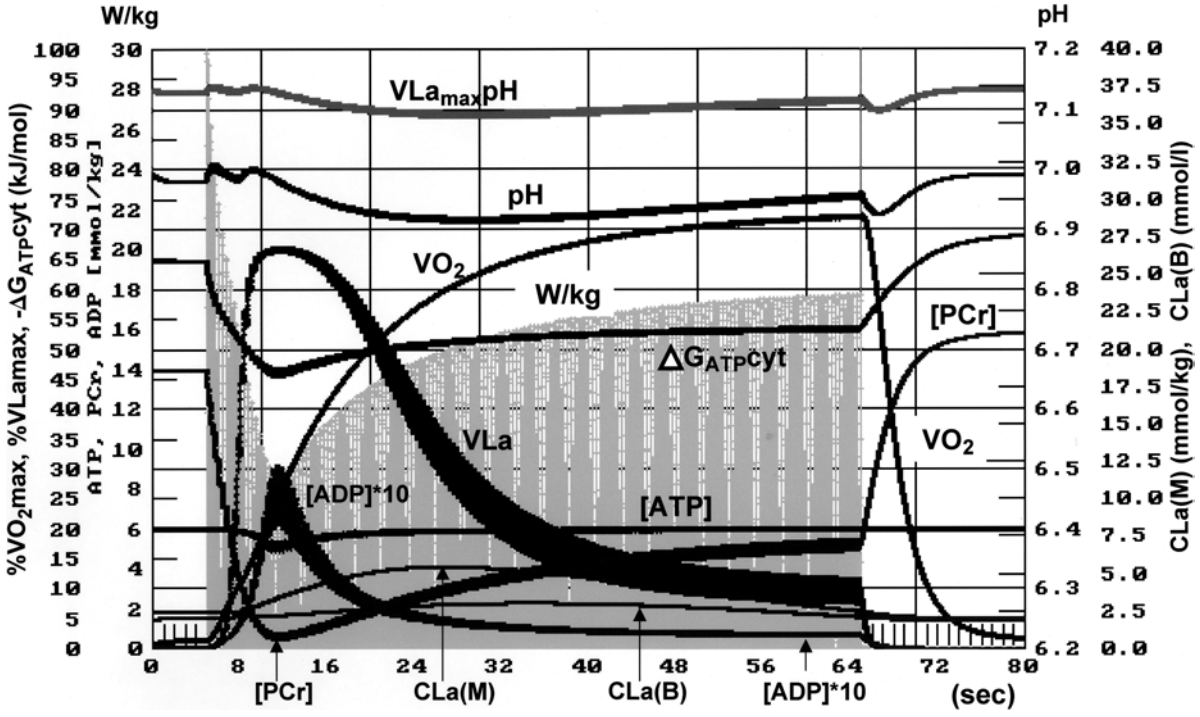

Fig. 8 Computer simulation of a sinus load (3.0 Hz = 180 beats·min^{-1}) on heart muscle at a power output corresponding to 70% of a virtual $\dot{V}O_{2max}$ of 1,000 ml·min^{-1}·kg^{-1}. At 70% of the virtual $\dot{V}O_{2max}$ the peak mechanical power is 90 W·kg^{-1} muscle. The VLa_{max} is assumed to be 0.5 mmol·s^{-1}·kg^{-1}, which is equivalent to the one sixth of the maximal oxidative power. The time constant for the adjustment of oxygen delivery (τ_s) to the tissue is assumed to be about 18 s. $\dot{V}O_2$ at rest is assumed to be 2.5 ml·min^{-1}·kg^{-1} muscle; Thus 70% of the total oxidative capacity represents an increase of 280 times the activity at rest. From the $\dot{V}O_2$ of 80 ml O_2·min^{-1}·kg^{-1} corresponding to a heart rate of 65 beat·min^{-1} to 70% $\dot{V}O_{2max}$ the change in power output is about eightfold leading to an increase of the heart minute volume from 5 to 30 l·min^{-1}. For more information and list of abbreviations see text

and [AMP]) and taking into account also the influence of the pH_m ($[H^+]$).

The rate of change of the instantaneous oxidative GP production can now be expressed with the aid of the second differential Eq. 19, which takes into account the time delay of the change of $\dot{V}O_2$ resulting from oxygen transport:

$$\mathbf{24)}\ \mathbf{d}[\mathbf{GP}]_{\dot{V}O2,a}/\mathbf{d}t = \mathbf{b}_{\dot{V}\mathbf{O2}} \times \mathbf{k}_{\dot{V}\mathbf{O2}} \times \{\dot{V}O_{2,max}/[\mathbf{1} + \mathbf{ks_1}/([\mathbf{ADP}] \times \Phi\Delta\mathbf{G}_{ADP})] - \dot{V}O_{2,a}\}\} \quad (24)$$

and where $\dot{V}O_{2,ss}$ is expressed as a function of [ADP] and $\Phi\Delta G_{ADP}$, as given by Eq. 13.

The differential Eqs. 23 and 24 can be solved numerically as time dependent functions of $\dot{V}O_{2,a,rest}$ and E. After each time interval, the current cytosolic equilibrium concentration of the CHEP system has to be recalculated using Eqs. 6, 7 and 8, including the influence of a possible change of $[H^+]$. Therefore Eqs. 23 and 24 contain an additional feedback from the change of $[la^-]_m$, the liberation of $[P]_i$ and the variation of PCO_2, which in turn results in a change of $[H^+]$. All these changes have a strong influence on the PCr-ATP equilibrium, as calculated from Eqs. 6 and 7, and on the activity of glycolysis, as from Eq. 16. An exact calculation of the resulting change in pH_m as function of the acid-base status might be possible but complex. However, an approximately correct linear relationship between the added base or acid equivalents and the change of pH_m can be calculated, using the the following equation:

$$\mathbf{25)}\ \mathbf{pH_m} = \mathbf{7.85} + \mathbf{d}_{buff} \times (\mathbf{0.8} \times [\mathbf{P}]_i - [la^-]_m) - \mathbf{0.55} \times \mathbf{log_{10}}(P\mathbf{CO_2}) \quad (25)$$

where the coefficient d_{buff} in the CS, was given a value of 54 mval·l^{-1}·pH_m^{-1}. In this way Eq. 25 combines the effects on pH_m of the various factors mentioned above. These will now be discussed separately.

It has been shown that there is a linear relationship between lactate concentration and pH_m within the physiological range of pH_m (Sahlin et al. 1975; Spriet et al. 1987b). The PCO_2 increases with $\dot{V}O_2$ as a result of increased CO_2 production. According to the Hasselbalch-Henderson equation, this increase has a direct influence on blood as well as on internal muscle pH_m. Despite the fact that a changing PCO_2 causes a change in bicarbonate towards a new PCO_2-bicarbonate equilibrium and in spite of the resulting delay in the established *steady state* PCO_2 at constant power output, the relationship between $\dot{V}O_{2,ss}$ and PCO_2 is roughly described by:

$$\mathbf{26)}\ P\mathbf{CO_2}(\mathbf{mmHg}) = \mathbf{40.0} + \mathbf{55} \times \dot{V}O_{2,a}/\dot{V}O_{2,max} \times (\mathbf{ml \cdot min^{-1} \cdot kg^{-1}}). \quad (26)$$

At an expected normal $\dot{V}O_{2max}$ of 120–160 ml·min^{-1}·kg^{-1} muscle, the maximal PCO_2 is calculated to be about 80 to 95 mmHg. The relationship between the PCO_2 and pH_m can be calculated by:

$$\mathbf{27)}\ \mathbf{pH_m = 7.736 - 0.55 \times \log_{10}[PCO_2(mmHg)]} \qquad (27)$$

for the dog skeletal muscle (Saborowski et al. 1971). In Eq. 25, the PCO_2 dependent influence on internal pH_m is given by the 2nd term on the right hand side of Eq. 27, $\Delta pH_m/\Delta \log PCO_2 = 0.55$. Therefore, Eqs. 25, 26 and 27 are part of the simulation model, to calculate the necessary feedback of the change of internal pH_m resulting from $[P]_i$ liberation, the influence of lactate accumulation and the change of PCO_2 brought about by the changes of $\dot{V}O_2$.

The term $v_{GP,E}$(millimoles per second per kilogram) corresponding to power output in Eqs. 18, 22 and 23 allows us to simulate the influence of a change of $\Delta G_{ATP,cyt}$ towards 0 on muscle strength and power output. The myosin ATPase is *inhibited* by the increase of free ADP and ceases to function if the cytosolic quotient of [ATP]/[ADP] falls below a certain level (Krause and Wegener 1996). A quasi-linear relationship between contraction force and $\Delta G_{ATP,cyt}$ has also been reported (Jeneson et al. 1995). The reduction of power output as function of a decreased phosphorylation state of the CHEP system can be calculated as a first approximation, by:

$$\mathbf{28)}\ \mathbf{F_{\Delta G} = cP}_E \times (\Delta G_{\mathbf{ATP},cyt} + \mathbf{39.5})/(-\mathbf{39.0}) \qquad (28)$$

where the term cP_E is an arbitrary conversion factor which is assigned a predetermined value such that the term $F_{\Delta G}$ under conditions of rest prior to exercise assumes a value of 1.0. During the following period of exercise $F_{\Delta G}$ decreases according to the decrease $\Delta G_{ATP,cyt}$, thus leading to a decreased power output which is larger the heavier the exercise. This mirrors the phenomenon of fatigue in the CS.

The factor cP_E can also be used to determine the difference in the maximal ATP turnover rate of fast or slow myosins which is known to be different by a factor of 3–5.

The AMP deaminase reaction has not been considered in this paper, because this requires another set of differential equations which makes it more difficult to demonstrate that the given solution of the high energy phosphate equilibrium within the regulatory circuit described by Eqs. 23 and 24 is exact and satisfies the conditions of an accurate regulation of glycolysis and OxP in the cell.

Lactate distribution in a two-compartment model

In humans and intact animals lactate exchange between the lactate producing active muscle tissue (active space) and a portion (fraction) of the extra cellular water space (passive space) can be described by a two-compartment model assuming that the main driving force is the concentration difference (Freund and Zoloumian 1981; Mader and Heck 1996). To describe the dynamic behaviour of lactate accumulation and removal, the differential equations must include $v_{la,ss,pH}$ in the active compartment, the net lactate exchange between the two compartments and the lactate elimination by oxidation and glycogen resynthesis. This leads to the following differential equations where the lactate concentration is calculated for each of the compartments:

$$\mathbf{29)}\ \mathbf{d}[la^-]_m/\mathbf{d}t = -\mathbf{K_1} \times ([la^-]_m - [la]_b) + \mathbf{1.35} * (v_{la,ss,pH} - v_{la,ox,m}) \qquad (29)$$

and

$$\mathbf{30)}\ \mathbf{d}[la]_b/\mathbf{d}t = V_{rel} \times \left[\mathbf{K_1} \times ([la^-]_m - [la^-]_b) - v_{la,ox,b}\right]. \qquad (30)$$

The $[la^-]_m$ and $[la^-]_b$ represent lactate concentration in the H_2O space of muscle and arterial blood, respectively. The factor $1.35 = 1/0.72$ accounts for the increase of concentration in the muscle H_2O space. The V_{rel} results from the quotient $\%V_m/\%V_b$ which is the ratio of the active lactate producing space to the passive lactate distribution space. The V_{rel} depends on the size of the active ($\%V_m$) and the passive ($\%V_b$) space, which can be expressed as percentage of the total body volume (100%). Based on experiments the available *lactate distribution space*, i.e. the sum of active and passive lactate space of the human body at rest, moderate or heavy exercise has been found to be about 30% to 50% of the total body space (Mader and Heck 1986; Searle and Cavalieri 1972). The two compartments are taken as representative (but virtual) spaces, which allow an approximately correct calculation of the energy yield from glycolysis, based on measurable concentrations time curves in blood and working muscles (Mader and Heck 1996).

Because of the lactate proton co-transport, the lower buffering capacity of blood and extra cellular space compared to muscle tissue leads to a steeper increase of $[H^+]$ in the blood which leads to a decreased speed of lactate exchange between muscle and blood with the increasing blood lactate concentration. Therefore the rate of lactate diffusion from muscle is nonlinearly related to the blood lactate concentration. As a first approximation, this is described by:

$$\mathbf{31)}\ \mathbf{K_1} = \mathbf{0.065} \times [la^-]_b^{\mathbf{-1.4}} \qquad (31)$$

The coefficient 0.065 and the exponent –1.4 are estimated from results in experiments on humans (Mader and Heck 1996) and the resulting *post exercise blood lactate concentration curves* in the simulation. The whole body lactate oxidation ($v_{la,ox}$) in animals or humans can be subdivided into $v_{la,ox,m}$ (two-thirds) and $v_{la,ox,b}$ (one-third), which represent the rates of oxidative lactate elimination from active and passive lactate spaces, respectively.

Application of the mathematical model

The theoretical description of the regulation of OxP and glycolysis summarized by the preceding equations has been coded in the programming language "C". The differential equations are integrated by iterative solution using a 5th-order Runge-Kutta-Fehlberg method (Engeln-Müllges and Reutter 1990). The CS of the dynamic changes of OxP and glycolysis as function of power output in watts per kilogram muscle were performed using a normal Pentium based PC. The diagrams yielded by the CS were plotted using the graphic software INGRAF (version 8.00. Integrated Graphics Library, Sugar Land, Tex., USA). In the paragraphs that follow, only a few examples of the simulation of the dynamic pattern of the metabolic behaviour will be reported. Numerous other simulations of exercise durations, ranging from the few seconds of a sprint to longer lasting exercise up to 30 min (Mader and Heck 1996; Mader 1998), have demonstrated that there are no restrictions in terms of time and mechanical power to the application of the model.

The metabolic response of the human body as a function of mechanical power output

A prerequisite for simulating the metabolic energy supply as a function of the mechanical power of the human body is knowledge of the ratio between active muscle mass and total body mass. The assumption that the muscle mass in normal young male athletes amounts to 35–45% of body mass, and that about 70%–80% of the muscle mass can be used in maximal efforts such as running, yields a working muscle mass of 25%–33% of body mass. The lactate distribution space is not equal to the *oxygen consuming space*, the latter being closely related to the active muscle mass. Therefore, the coefficient relating average $\dot{V}O_2$ in the working muscle mass to total body mass is different from that relating lactate space to total body space (Mader and Heck 1986, 1996). The transformation coefficient from body mass to active muscle mass therefore varies between 100%/25% = 4 and 100%/33% = 3.0. All the CS in this paper are based on 1.0 kg muscle mass.

In vitro 1.0 ml V_{mit} can consume up to 4.5 ml $O_2 \cdot min^{-1}$ (Hoppeler 1990; Rumsey et al. 1990; Mootha et al. 1997). Since the normal human skeletal muscle contains about 3.5% mitochondria, $\dot{V}O_{2max}$ can be calculated to be 158 $ml \cdot min^{-1} \cdot kg^{-1}$ muscle. If it is assumed that the P/O-quotient is 2.6, corresponding to a requirement of 11.2 ml O_2 by 2.6 mmol ATP equivalent to 4.3 ml O_2 for the production of 1.0 mmol ATP, the above calculated $\dot{V}O_{2max}$ is equivalent to a production rate of about 0.6 mmol $PCr \cdot s^{-1} \cdot kg^{-1}$ muscle. For a physical education student of 70 kg body mass, and 30% body mass as active muscle, $\dot{V}O_{2max}$ is assumed to be 3,300 $ml \cdot min^{-1}$. Together with a $\dot{V}O_2$ of about 400 $ml \cdot min^{-1}$ at rest this amounts to 3,700 $ml \cdot min^{-1}$ (about 53 $ml \cdot min^{-1} \cdot kg^{-1}$ body mass). The PCr-content is assumed to be about 24 $mmol \cdot kg^{-1}$ muscle. The $v_{la,max}$ is assumed to be about 1.0 $mmol \cdot s^{-1} \cdot kg^{-1}$ which is equivalent to 0.5 $mmol \cdot s^{-1} \cdot kg^{-1}$ glucose turnover during maximal activation of glycolysis (Spriet et al. 1987a).

In the CS (Fig. 5) at a *supra maximal load*, the first rapid exponential response of $\dot{V}O_2$, up to 70% of the peak $\dot{V}O_2$, is followed by an approximately linear increase until the cessation of exercise. This is consistent with observations in many experiments and as reported in some papers (e. g. Barstow et al. 1993) it is difficult to give a plausible explanation of this phenomenon purely from the point of view of the experiment. However, this non *steady state* behaviour of $\dot{V}O_2$, can be easily explained if it is considered to be a consequence of the decline of the ATP production by $v_{la,ss,pH}$, caused by the inhibition of glycolysis resulting from the accumulation of lactate. The slight continuing decrease of the phosphorylation state of the CHEP system leads to the decline in power output and the increase of free [ADP]. The inhibition of glycolysis shifts ATP production to the oxidative side. The $\dot{V}O_{2max}$ occurs at the stage of a complete breakdown of [PCr].

In the CS of Fig. 6 an overall oxidative steady state is achieved at about 60% of $\dot{V}O_{2max}$ and low levels of steady-state muscle and blood lactate (Mader and Heck 1986; Mader 1999). The lactate steady state results from $v_{la,ss,pH}$ and the adjustment of lactate oxidation by increasing $[la^-]_m/[la^-]_b$, as calculated by Eq. 17 (Mader 1999). In this case the *oxygen deficit* can be calculated by a mono exponential rise of the $\dot{V}O_2$ with only a small error. In Figs. 5 and 6 the CS are based on real changes of $\dot{V}O_{2,rest}$ up to peak-$\dot{V}O_2$, close to the $\dot{V}O_{2max}$ evaluated in the ergometer trials and related to the stage of the muscle fatigue caused by the depletion of [PCr] and a decline of [ATP] (Barstow et al. 1993, 1994; Kent-Braun et al. 1993; Sahlin et al. 1975; Spriet et al. 1987a; Taylor et al. 1986).

The metabolic response of muscles with an extremely high oxidative capacity

It has been suggested that $\dot{V}O_2$ and ATP production in muscles with a mitochondria content of more than 25%, such as the flight muscles of humming birds or the mammalian heart, in vivo, are regulated differently when compared to the more usual low oxidative skeletal muscles (Balaban 1990; Balaban and Heineman 1989; Heineman and Balaban 1990; Hochachka and Matheson 1992; Hochachka and McLelland 1997). As for the heart muscle, the CS in Fig. 7 shows that the PCr content at the *steady state* does not change, but oscillates slightly during a cycle of systole and diastole at the normal frequency of the human heart at rest (65 $beats \cdot min^{-1}$, $\dot{V}O_2$ about 8 $ml \cdot min^{-1} \cdot 100g^{-1}$ or 17% of the observed $\dot{V}O_{2max}$). This agrees with the results of ^{31}P-NMR-spectroscopy of the heart muscle in animal experiments (Kantor et al. 1986). However, the speculation that the

"lack of variation of high-energy phosphorylated species suggest a tight coupling between energy production and consumption, with the maximum ATP-production during peak systole" (Kantor et al. 1986) is not a crucial one.

The CS calculated relation of [PCr]:[ATP] = 2.05 during normal activity at rest is nearly the same as that observed in the heart muscle in vivo (about 1.9 ± 0.1) in animal experiments. However, the corresponding content of free [ADP] has been found to be five times lower in the CS compared to the experimental data (Balaban and Heineman 1989; Balaban et al. 1986; Kantor et al. 1986; Katz et al. 1988a, 1989; Lewandowski et al. 1987). This high level of free [ADP] is mainly due to a large excess of free [Cr] compared to the assumed $[P]_i$ (Balaban et al. 1986; Balaban 1990; Katz et al. 1988b, 1989). For example, in one of the key papers (Katz et al. 1989) the total content of creatine compounds is determined to be 27.3 $mmol \cdot l^{-1}$ H_2O, and [ATP] is assumed to be 6.6 $mmol \cdot l^{-1}$. With a [PCr]:[ATP] ratio of 2.0 under normal activity at rest the calculated [PCr] is 13.65 $mmol \cdot l^{-1}$. Thus an equal amount of [Cr] is unphosphorylated. This excess of free [Cr] could not be phosphorylated because of the assumed very low free $[P]_i$ (about 1.2 $mmol \cdot l^{-1}$) leading to a [PCr]:$[P]_i$ ratio of 12.5. Using a free $[P]_i$ of about 1.5 $mmol \cdot l^{-1}$ ([PCr]:$[P]_i$ of about 9) in the CS, then 17% of $\dot{V}O_{2max}$ can be achieved with free [ADP] of about 0.01 $mmol \cdot l^{-1}$ together with the reported $\Delta G_{ATP,cyt}$ of about –61 $kJ \cdot mol^{-1}$ (see Fig. 3). So free cytosolic [ADP] in the heart is kept very low under normal functional conditions.

The maximal rate of $\dot{V}O_2$ of 1.0 ml V_{mit} from heart muscle, as measured in a suspension of about 0.01 ml $V_{mit} \cdot ml^{-1}$ H_2O, amounts to about 4.5 $ml^{-1} \cdot min^{-1}$ $O_2 \cdot ml^{-1}$ V_{mit} (Mootha et al. 1997). Extrapolation of this value to the intact heart on the basis of a mitochondria content of about 22% leads to a virtual (but not real) $\dot{V}O_{2max}$ of 100 ml $O_2 \cdot min^{-1} \cdot 100g^{-1}$ (or 1,000 $ml \cdot min^{-1} \cdot kg^{-1}$). This constitutes a speculated 300-fold increase in the rate of OxP from cardiac arrest with an assumed $\dot{V}O_2$ of 3.0 $ml \cdot min^{-1} \cdot kg^{-1}$ to maximal power output (Hochachka and Matheson 1992; Hochachka and McLelland 1997). However, the real changes of $\dot{V}O_2$ are presumably considerably lower.

In human hearts between normal frequencies at rest of 65 $beats \cdot min^{-1}$ and at maximal of 190 $beats \cdot min^{-1}$ the $\dot{V}O_2$ increases about eightfold from 8.0 to about 65 $ml \cdot min^{-1} \cdot 100g^{-1}$. Similarly, in the canine heart the myocardial $\dot{V}O_2$ at rest was measured at about 4.1 ml $O_2 \cdot min^{-1} \cdot 100g^{-1}$ (Katz et al. 1989). The observed maximal increase in $\dot{V}O_2$ was about 12-fold, i.e. up to about 50 ml $O_2 \cdot min^{-1} \cdot 100g^{-1}$. This suggests that the actual $\dot{V}O_{2max}$ of the heart, related to the mitochondria density in the cardiac myocytes, is dictated by the principle of biological similarity, as described by:

$$\mathbf{32)}\ \dot{V}O_{2,max}(\mathbf{ml \cdot min^{-1} \cdot ml^{-1}}\ V_{mit}) = \mathbf{4.5} * \mathbf{\%} V_{mit}^{\mathbf{-0.15}}. \quad (32)$$

Hemmingsen (1960).

On the basis of this equation, the maximal rate of OxP of the myocardium which can be maintained for 2 min is reduced from 4.5 to about 2.8 ml $O_2 \cdot min^{-1} \cdot ml^{-1}$ V_{mit}. This is about 60% to 65% of the expected (virtual) $\dot{V}O_{2max}$ and agrees well with the upper limit of the experimentally obtained values. The metabolic rate of a non-contracting heart muscle was experimentally determined to be approximately three times the metabolic rate of the soleus muscle at rest (Loiselle 1987). This puts the limit of the maximal possible changes of the metabolic rate of OxP from cardiac arrest to $\dot{V}O_{2max}$ to a maximum of 100-fold.

The CS of Fig. 8 shows the well-known transient "staircase behaviour of the contraction amplitude" of the heart muscle which is usually observed in experiments on isolated hearts from a stage of low activity, or cardiac arrest, to that approaching a steady-state contraction amplitude (Mast and Elzinga 1987) at about 70% of the (virtual) $\dot{V}O_{2max}$. Contraction force and power output are calculated as a function of $\Delta G_{ATP,cyt}$ using Eq. 28. The transient behaviour of the model parameters is as complex as in the real heart. The time constant $\tau_{\dot{V}O2}$ for a delay of OxP calculated using Eq. 19 or 24 is set to 1.0 s, and is due to intracellular adjustments of OxP. The real time constant for establishing a sufficient oxygen delivery in the tissue under these conditions is about 20 s (Korecky and Brandejs-Barry 1987). This is simulated by an exponential increase of the $\dot{V}O_{2max,ap}$ after the start of exercise, approaching real $\dot{V}O_{2max}$ calculated from Eq. 32, as described by:

$$\mathbf{33)}\ \dot{V}O_{2,max,ap} = \dot{V}O_{2,max} \times (\mathbf{1} - \mathbf{e}^{-t/\mathbf{18}}). \quad (33)$$

The *steady state* of $\dot{V}O_2$ and of contraction amplitude in the CS is attained after more than 60 s. A transient decrease of [PCr] to a low level of 2.0 $mmol \cdot kg^{-1}$ is also observed, together with a transient high activation of glycolysis (about 65% of $v_{la,max}$ and equal to 0.5 $mmol \cdot s^{-1} \cdot kg^{-1}$) which keeps contraction force relatively high, and disappears with the relatively slow increase of $\dot{V}O_2$ to the steady-state $\dot{V}O_2$. Glycolysis oscillates with the cardiac cycle to about $\pm 3\%$ of the average remaining activation (about 10%) at the steady-state OxP (see Fig. 9). In Figs. 8 and 9 the CS calculated ratio of [PCr]:[ATP] below 1.0 is related to about a tenfold increase of $\dot{V}O_2$ compared to normal activity at rest in canine hearts (Loiselle 1987). A ratio of [PCr]:[ATP] of about 1.2 is observed in rat hearts under normal working conditions (Katz et al. 1988a), where not much of a further increase of $\dot{V}O_2$ can be expected. This agrees also with the behaviour of hearts in vitro (Kantor et al. 1986; Katz et al. 1989; Lewandowski et al. 1987).

The [PCr]:[ATP] ratio under external pacing and adrenaline stimulation in real hearts varies from 1.7 to 1.3, being essentially constant for each experimental animal (Balaban et al. 1986; Heineman and Balaban 1990; Katz et al. 1989). In the CS a twofold increase of

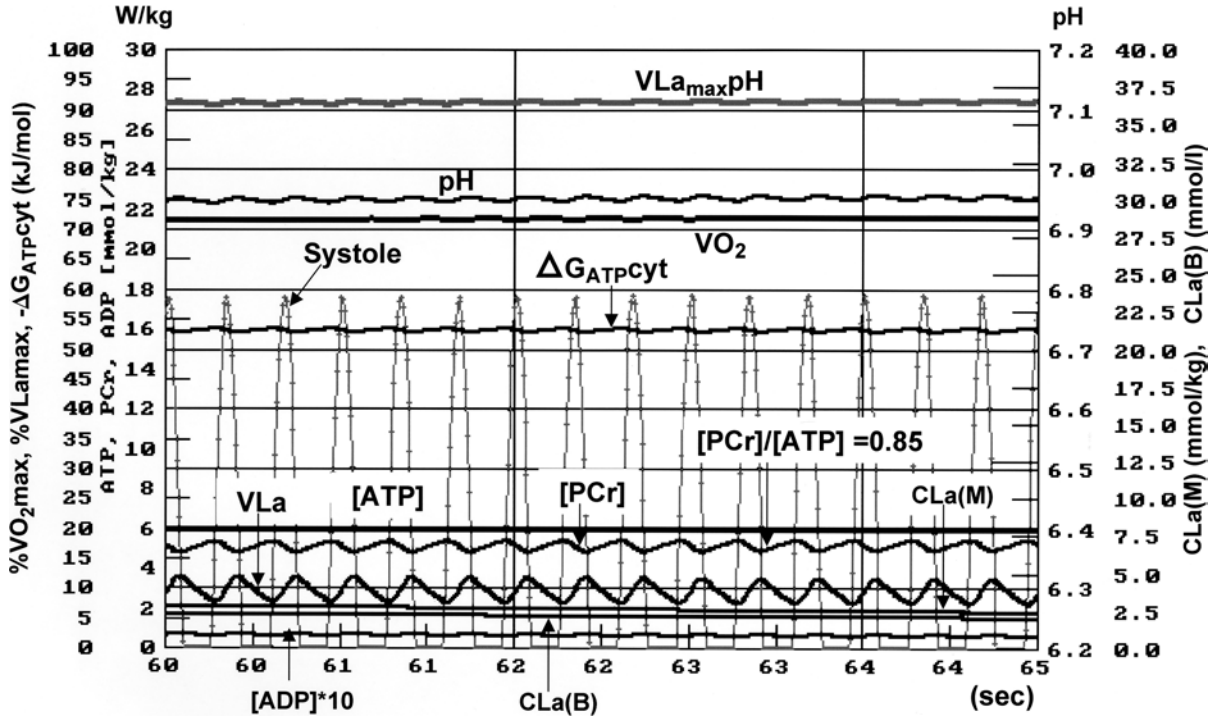

Fig. 9 Selective enlargement of part of Fig. 8 (60–65 s, 3.0 Hz repeated contraction, sinus load). In spite of an approximately 90 W·kg^{-1} peak power output per beat the *PCr*-content remains approximately constant at 5.0 mmol·kg^{-1}. Glycolysis exhibits oscillations of about one-third of the average activity of 12% of VLa_{max}, which contributes to the buffering of [PCr] during the contraction relaxation cycle. From normal to maximal activity the [PCr] decrease is 7.0 mmol·kg^{-1}. For list of abbreviation see text

$\dot{V}O_2$ leads to a [PCr]:[ATP] ratio of 1.75 corresponding to an established steady-state $\dot{V}O_2$ of about 30% of a virtual $\dot{V}O_{2max}$, related to 26% V_{mit}. This is within the range of the observations in experiments (Balaban et al. 1986). At about 40% of the assumed virtual $\dot{V}O_{2max}$ the *steady state ratio* of [PCr]:[ATP] is about 1.6 which indicates that in a medium range of OxP the CS yields a high phosphorylation state. Thus, it appears that a gap remains between the CS and the real behaviour of hearts in vivo during adrenaline stimulation. This is probably due to the *inotropic effect*, which is not considered in the presented model. However, this is consistent with the basic assumptions of the model and needs only to be implemented. Indeed, if it is assumed that adrenaline leads to an increase of Δp and of its equivalent $\Delta G_{ox,ap}$, this effect might explain the observed difference of the [PCr]:[ATP] ratio between hearts driven in vivo under adrenaline stimulation and the CS. In the low range of free [ADP], below 50% of $\dot{V}O_{2max}$, according to Eqs. 9 and 13 the effect of an increase of $\Delta G_{ox,ap}$ of –5,0 kJ·mol^{-1} is equivalent to a five- to eightfold increase of free [ADP]. That this may indeed be the case is also suggested by experimental data, which has shown that the NADH/NAD$^+$ redox state can alter the rate of OxP of isolated mitochondria and that the increase in submaximal respiratory rate induced by pyruvate excess can occur without large alterations in free [ADP], $[P]_i$ and [ATP] (Barstow et al. 1993; Koretsky and Balaban 1987).

Finally, in Fig. 10 it is demonstrated that the theoretical scheme developed above applies also to the minimal conditions of the CHEP system of living skeletal muscle cells. Using creatine analogues, the PCr content of muscle cells is reduced to 1/3–1/4 of the normal values (Korecky and Brandejs-Barry 1987; Meyer 1988). The behaviour of the experimentally obtained transients of OxP and [PCr] from rest (about 6.0 mmol·kg^{-1}) to steady state (about 1.8 mmol·kg^{-1}) and in recovery (Meyer 1989) can be re-simulated very precisely.

General aspects of the regulation of OxP

The failure to provide a satisfactory explanation of the regulation of OxP, as deduced from experimental results, is to some extent due to a lack of consistent quantitative calculations of known regulating factors and functions. Data from ^{31}P-NMR spectroscopy show that the values of free [ADP], within the concentration range in which OxP and glycolysis are proposed to be regulated, are far below the 0.2 mmol·kg^{-1} wet mass which is the limit for a direct determination in muscle biopsy samples and in ^{31}P-NMR spectroscopy (Arnold et al. 1984; Connett and Honig 1989; Kushmerick 1987; Kushmerick et al. 1992; Sahlin et al. 1975). Consequently, one of the major sources of the discrepancies in the interpretation of the experimental data in the literature arises from the calculation of free [ADP].

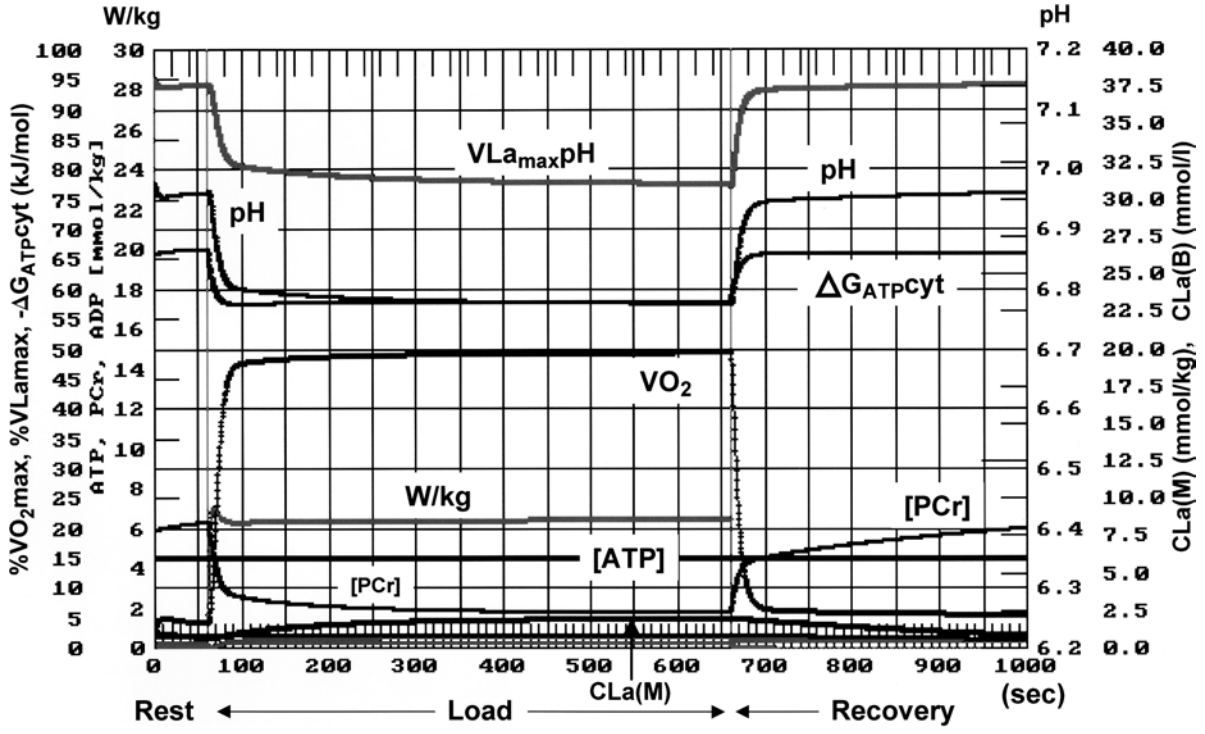

Fig. 10 Computer simulation of animal experiments using creatine analogues for reducing *[PCr]* to 25% of the normal PCr content. The experiment is reported at the stage of 6 weeks using creatine analogues and is recalculated. With the exception of a small transient overshoot the simulated parameters fit the results of the experiment. For abbreviations see list

Indeed, as explained above, it is difficult to make exact calculations of free [ADP] in this range of concentrations from measurements of [Cr] and [ATP] and of the ratio of [ATP] to [PCr], as has commonly been done (Balaban et al. 1986; Conley et al. 1997; Connett and Honig 1989; Heineman and Balaban 1990; Katz et al. 1989; Kushmerick 1987; Kushmerick et al. 1992). Free [Cr] is determined frequently to be in large excess, compared to free $[P]_i$. This excess of [Cr] over $[P]_i$ adds a relatively large base source of calculated free [ADP] to the possible functional changes of free [ADP] which are restricted to values of $[P]_i$ greater than 0. The calculated additional changes of free [ADP] are also rather small and seem negligible (Balaban 1990; Balaban and Heineman 1989; Connett and Honig 1989; Heineman and Balaban 1990; Katz et al. 1989). If, however, the calculation is based on free $[P]_i$ (Barstow et al. 1994; Chance et al. 1985a, b) or with only a small excess of [Cr] over $[P]_i$ (Arnold et al. 1984; Kushmerick et al. 1992; Nioka et al. 1992; Taylor et al. 1986), then small changes in free [Cr] will cause large changes in the content of free [ADP] calculated from Eq. 2. In this case, the calculated change of free [ADP] in vivo fits well with the known $Km(0.5) = 0.035 \pm 0.01$ mmol·l^{-1} for the 50% activation of $\dot{V}O_2$ (Arnold et al. 1984; Barstow et al. 1994; Chance et al. 1985b; Kushmerick et al. 1992; Nioka et al. 1992; Taylor et al. 1986). Thus, it seems that the only way to overcome this problem is to calculate the PCr-ATP equilibrium using free $[P]_i$ under in vivo conditions instead of free [Cr].

One of the main points of disagreement stems from the assumption that free cytosolic [ADP] drives OxP as a key substrate according to the MM-kinetic model. This is a difficult question because free cytosolic [ADP] is separated from the ATP-generating F_0/F_1-ATPase complex by the inner mitochondrial membrane; therefore only free $[ADP]_{mit}$ together with $[P]_{i,mit}$ inside the mitochondrial space are the key substrates for ATP-production (see Fig. 4). The $[ATP]_{mit}$:$[ADP]_{mit}$ ratio is not greatly dependent on pH in the matrix space, so that pH does not affect this ratio, according to Eq. 4. According to Eq. 10 it is assumed, that the F_0/F_1-ATPase complex generates a $\Delta G_{ATP,mit}$ below $3 \times -22 = -66$ kJ·mol^{-1}, because the reaction is potentially irreversible. However, the $[ATP]_{mit}$:$[ADP]_{mit}$ ratio at state 4 and 3 respiring mitochondria was experimentally determined to be 10 up to 20 times lower compared to the cytosol (Erecinska and Wilson 1982; Klingenberg 1980; Soboll 1995). If the cytosolic and the mitochondrial ATP:ADP-ratio differ by a factor of 10 or more, this rules out the possibility that OxP is directly driven by free cytosolic [ADP]. The same applies to the exchange of ADP compared to ATP by the adenine nucleotide translocase which in this case is also not driven by concentration differences of free [ADP] (Erecinska and Wilson 1982; Klingenberg 1980; Soboll 1995; Williamson 1979; Wilson et al. 1983). The only conclusion therefore is that a difference of *potentials* rules the rate of OxP and determines free [ADP] in the cytosol. If this is so, $\Delta G_{ox,ap}$ which appears at the cytosolic side as driving force related to the $\Delta p'$ must be a

composite of a low $\Delta G_{ATP,mit}$ resulting from a low $[ATP]_{mit}$:$[ADP]_{mit}$ ratio and an additional driving force generated at the level of the ATP^{-4}/ADP^{-3} translocase (Ferguson 2000). As the ionic exchange by the ATP^{-4}/ADP^{-3} and OH^-/P_i^{2-} translocators together with H^+ is 0 an additional –22 kJ·mol^{-1} is available to overcome the difference of a lower $\Delta G_{ATP,mit}$ against $\Delta G_{ATP,cyt}$ and to drive ADP transfer to mitochondria against the concentration difference of low free cytosolic [ADP] to higher $[ADP]_{mit}$ (see Fig. 4). That the rate of ADP-ATP exchange across the inner mitochondrial membrane can be modified or driven by potential differences was demonstrated by Klingenberg (1980).

On the other hand it is unlikely that $[ADP]_{mit}$ is high at rest so that it does not change more than four times between OxP at rest (about 0.05 mmol·l^{-1}) and $\dot{V}O_{2max}$ (0.2 mmol·l^{-1}). Furthermore, it is also unlikely that the F_0F_1-ATPase complex is maintained always at a high saturation level by its substrate ADP – which indeed is the case – but that a change of $\Delta p'$ cannot influence $\Delta G_{ATP,mit}$. This last point is indeed at variance with the experimental observation that $\Delta G_{ATP,cyt}$ can achieve up to –70 kJ·mol^{-1} during recovery from heavy exercise calculated from ^{31}P-NMR spectroscopy experiments (Wackerhage et al. 1998). Since the calculations of a low $[ATP]_{mit}$:$[ADP]_{mit}$ ratio are in all cases based on chemical determinations of $[ADP]_{mit}$ after rapid deproteination and clamp freezing, the inner mitochondrial phosphorylation state may be deteriorated by this process. The chemically determined $[ADP]_{mit}$ contains a tightly bonded ADP/P_i fraction from the F_0/F_1-ATPase complex, amounting to 14% of the protein content of the inner mitochondrial membrane. The chemically obtained results may not, therefore, represent the real $[ATP]_{mit}$:$[ADP]_{mit}$ ratio. In addition, new experimental results indicate that the 3:1 coupling of proton to ATP formation is not as fixed as commonly believed (Ferguson 2000). So the free $[ADP]_{mit}$ together with free $[P]_{i,mit}$ can be kept low and $\Delta G_{ATP,mit}$ may approach $\Delta G_{ATP,cyt}$ under conditions of rest. If, according to Elston et al. (1998), four protons are transferred to produce one ATP, Eq. 11 would indicate that $\Delta G_{ATP,mit}$ could be in the range of –60 to –70 kJ·mol^{-1}, i.e. equal to $\Delta G_{ATP,cyt}$ at rest. Since the $\Delta p'$ is kept relatively constant even with an increasing rate of OxP up to $\dot{V}O_{2max}$, $\Delta G_{ATP,mit}$ is also kept high. If, however, the $[ATP]_{mit}$:$[ADP]_{mit}$ ratio as a function of $\Delta p'$ is not so much below the cytosolic [ATP]:[ADP] ratio even under conditions of rest it is not necessary to give up the idea that OxP is controlled via the MM kinetic, regulated by the level of the free [ADP]. In this case indeed, ADP does not need to be transported against a high concentration difference. This also was first concluded by Williamson (1979).

If, however, free $[ADP]_{mit}$ together with $[P]_{i,mit}$ is kept at a low level by a high affinity of the F_0/F_1-ATPase complex for both substrates which mirrors $\Delta p'$ at high $\Delta G_{ATP,mit}$, then the assumption that the free cytosolic [ADP] directly drives the exchange rate in part at the level of the ATP^{-4}/ADP^{-3} translocase is very likely. Under these assumptions the regulation concept of OxP from the cytosolic side is simple and clear. The equivalent of the *apparent* $\Delta p'$ ($\Delta G_{ox,ap}$) reflects the driving force of OxP from the mitochondrial side according to Eq. 11 and Eq. 13 is to some extent a causal but simplified mathematical description of this process which determines the degree of the activity of OxP from the cytosolic side.

In this paper the model is limited to the cytosolic side of OxP with the assumption of a constant $\Delta G_{ox,const}$ of –72.5 kJ·mol^{-1}. This is the *equilibrium point* at which the rate of OxP, as calculated by Eq. 13, equals 0. This first approach neglects existing changes of the *apparent* $\Delta p'$ observed in experiments. At every stage of activity of OxP, even at rest, a deviation from the equilibrium related to a $\Phi\Delta G_{ADP}$ greater than 0 is necessary to keep the system working. Indeed, a complete equilibrium cannot be reached because of the existence of a *basic oxidation rate* of 0.5 ml O_2·min^{-1}·kg^{-1} or more in normal skeletal muscles, related to the *proton leak* of the inner mitochondrial membrane and the heat production necessary to maintain body temperature at 37°C (Loiselle 1987; Rolfe and Brown 1997). At complete equilibrium no fluxes can exist. It is thus clear that increasing fluxes need increasing driving forces and increasing substrate or activator concentrations which must deviate from the equilibrium status close to resting conditions.

In summary the proposed concept of regulation is a basic approach at the simplest possible level; it can be taken as an attempt to integrate the two main disagreeing concepts of the regulation of OxP in vivo from the past. Results from the CS demonstrate a high level of similarity with the experimentally observed dynamic behaviour of measurable parameters of OxP, glycolysis and the behaviour of the parameters of the CHEP system. The advantage of a complete simulation of the behaviour of OxP and glycolysis as function of the energy demand of muscle cells is that the model also calculates from a clear theoretical base the details of the parameters that can be measured in various experimental situations. Furthermore, the CS shows that complex dynamic behaviour in real biological systems can be ruled by a few general principles and a relatively simple set of equations. It is, however, clear that the model needs a more detailed implementation of the characteristics of the reactions occurring at the site of the mitochondria. This however does not change the calculation of the main regulation of OxP and glycolysis as explained in this paper.

Acknowledgement The financial support of the Ministry of Schools, Education and Research of Nordrhein Westfalen, Germany, is gratefully acknowledged. The scientific advice and help of Professor Doctor Pietro E. di Prampero in improving the shape and style of the manuscript are gratefully acknowledged.

References

Arnold DL, Matthews PM, Radda GK (1984) Metabolic recovery after exercise and the assessment of mitochondrial function in vivo in human skeletal muscle by means of ^{31}P-NMR. Magn Reson Med 1:307–315

Balaban RS (1990) Regulation of oxidative phosphorylation in the mammalian cell. Am J Physiol 258:C377-C389

Balaban RS, Heineman FW (1989) Control of mitochondrial respiration in the heart in vivo. Mol Cell Biochem 89:191–197

Balaban RS, Kantor HL, Katz LA, Briggs RW (1986) Relation between work and phosphate metabolite in the in vivo paced mammalian heart. Science 232:1121–1123

Barstow TJ, Casaburi R, Wasserman K (1993) O_2 uptake kinetics and the O_2 deficit as related to exercise intensity and blood lactate. J Appl Physiol 75:755–762

Barstow TJ, Buchtal SD, Zancanotto S, Cooper DM (1994) Changes in the potential Controller of human skeletal muscle respiration during incremental calf exercise. J Appl Physiol 77:2169–2176

Brown GC (1992) Control of respiration and ATP synthesis in mammalian mitochondria and cells. Biochem J 284:1–13

Chance B, Williams GR (1955) Respiratory enzymes in oxidative phosphorylation. I. Kinetics of oxygen utilization. J Biol Chem 217:383–393

Chance B, Clark BJ, Nioka S, Subramanian H, Maris JM, Argov Z, Bode H (1985a) Phosphorus nuclear magnetic resonance spectroscopy in vivo. Cardiovascular metabolic imaging. Circulation 72 [Suppl IV]:103–110

Chance B, Leigh JS, Kent J, McCully K (1985b) Metabolic control principles and ^{31}P-NMR. Fed Proc 82:8384–8388

Cieslar JH, Dobson GR (2000) Free [ADP] and aerobic muscle work follow at least second order kinetcs in rat gastrocnemius in vivo. J Biol Chem 275:6129–6134

Conley KE, Blei ML, Richards TL, Kushmerick MJ, Jubrias SA (1997) Activation of glycolysis in human muscle in vivo. Am J Physiol 273:C306–C315

Connet TRJ (1988) Analysis of metabolic control: new insights using scaled creatine kinase model. Am J Physiol 254:R949–R959

Connett RJ, Honig CR (1989) Regulation of VO_2 in red muscle: do current biochemical hypotheses fit in vivo data? Am J Physiol 256:R898–R906

Danforth WH (1965) Activation of glycolytic pathway in muscle. In: Chance B, Estabrook RW, Williamson JR (eds) Control of energy metabolism. Academic Press, New York, pp 287–297

Donovan CM, Brooks GA (1983) Endurance training effects lactate clearance not lactate production. Am J Physiol 244:E83–E92

ElstonT, Wang H, Oster G (1998) Energy transduction in ATP synthase. Nature 391:510–513

Engeln-Müllges G, Reutter F (1990) Formelsammlung zur Numerischen Mathematik mit C-Programmen. BI-Wissenschaftsverlag, Mannheim

Erecinska M, Wilson DF (1982) Regulation of cellular energy metabolism. J Membr Biol 70:1–14

Ferguson S (2000) ATP-synthetase: what dictates the size of a ring? Curr Biol 10:R804–R808

Fontaine EM, Devin A, Rigoulet M, Leverve XM (1997) The yield of oxidative phosphorylation is controlled both by force und flux. Biochem Biophys Res Commun 232:532–535

Freund H, Zouloumian P (1981). Lactate after exercise in man. I. Evolution kinetics in arterial blood. Eur J Appl Physiol 46:121–133

Funk CI, Clark A, Connett RJ (1990) A simple model of aerobic metabolism: application to work transitions in muscle. Am J Physiol 258:C995–C1005

Golding EM, Teague WE, Dobson GP (1995) Adjustment of K' to varying pH and pMg for the creatine kinase, adenylate kinase and hydrolysis equilibria permitting quantitative bioenergetic assesment. J Exp Biol 198:1775–1782

Hansford RG, Zorov D (1998) Role of mitochondrial calcium transport in the control of substrate oxidation. Mol Cell Biochem 184:359–369

Heineman FW, Balaban RS (1990) Phosporus-31 nuclear magnetic resonance analysis of transient changes of canine myocardial metabolism in vivo. J Clin Invest 85:843–852

Hemmingsen AM (1960) Energy metabolism as related to body size and respiratory surfaces, and its evolution. Rep Steno Mem Hosp, IX/Part II, Copenhagen

Hochachka PW, Matheson GO (1992) Regulating ATP-turnover rates over broad dynamic work ranges in skeletal muscles. J Appl Physiol 73:1697–1703

Hochachka PW, Mclelland G (1997) Cellular metabolic homeostasis during large- scale change in ATP turnover rates in muscle. J Exp Biol 200:381–386

Hoppeler H (1990) The different relationship of VO_2max to muscle mitochondria in humans and quadrupedal animals. Respir Physiol 80:137–146

Jeneson JA, Westerhoff HV, Brown TR, Van Echteld CJ, Berger R (1995) Quasi-linear relationship between Gibbs free energy of ATP hydrolysis and power output in human forearm muscle. Am J Physiol 268:C1474–C1484

Kantor HL, Briggs RW, Metz KR, Balaban RS (1986) Gated in vivo examination of cardiac metabolites with ^{31}P nuclear magnetic resonance. Am J Physiol 251:H171–H175

Katz LA, Koretsky AP, Balaban RS (1988a) Activation of dehydrogenase activity and cardiac respiration: a ^{31}P-NMR study. Am J Physiol 255:H185–H188

Katz LA, Swain JA, Portman MA, Balaban RS(1988b) Intracellular pH and inorganic phosphate content of heart in vivo: a ^{31}P-NMR study. Am J Physiol 255:H189–H196

Katz LA, Swain JA, Portman MA, Balaban RS (1989) Relation between phosphate metabolites and oxygen consumption of heart in vivo. Am J Physiol 256:H265–H274

Kent-Braun JA, Miller RG, Weiner MW (1993) Phases of metabolism during progressive exercise to fatigue in human skeletal muscle. J Appl Physiol 75:573–580

Klingenberg M (1980) The ADP-ATP translocation in mitochondria, a membrane potential controlled transport. J Membr Biol 56:97–105

Korecky B, Brandejs-Barry Y (1987) Effect of creatine depletion on myocardial mechanics. In: Jacob R, Just H, Holubarsch C (eds) Cardiac energetics – basic mechanism and clinical implications. Springer, Berlin Heidelberg New York, pp104–110

Koretsky AP, Balaban RS (1987) Changes in pyridine nucleotide levels alter oxygen consumption and extra mitochondrial phosphates in isolated mitochondria: a ^{31}P-NMR and NAD(P)H fluorescence study. Biochim Biophys Acta 893:398–408

Krause U, Wegener G (1996) Control of adenine nucleotide metabolism and glycolysis in vertebrate skeletal muscle during exercise. Experientia 52:396–403

Kushmerick MJ (1987) Energetics studies of muscles of different types. Basic Res Cardiol 82 [Suppl 2]:17–30

Kushmerick J, Meyer RA, Brown TR (1992) Regulation of oxygen consumption in fast and slow-twich muscle. Am J Physiol 263:C598–C606

Lewandowski ED, Devous MD Sr, Nunnally RL (1987) High-energy phospates and function in isolated, working rabbit hearts. Am J Physiol 253:H1215–H1223

LeRumeur, E, LeTallec N, Kernec F, Certalnes JD (1997) Kinetics of ATP to ADP beta-phosphoryl conversion in contracting skeletal muscle by in vivo ^{31}P-NMR magnetization transfer. NMR Biomed 10:67–72

Loiselle DS (1987) Cardiac basal and activation metabolism. In: Jacob R, Just H, Holubarsch C (eds) Cardiac energetics – basic mechanism and clinical implications. Springer, Berlin Heidelberg New York, pp 37–50

Mader A (1998) Die Simulation der Dynamik des Energiestoffwechsels der Muskelzelle – Praktische Anwendung zur Interpretation experimenteller Befunde der physiologischen

Grundlagen Forschung und der Humanleistungsphysiologie. In: Mester J, Perl J (eds) Informatik im Sport. Bundesinst Sportwiss 5:99–115

Mader A (1999) Anaerobic threshold (AT) as determined by VO_2max and VLA_{max} of the working muscle mass of the human body. An update of the theoretical concept. In: Parisi P, Pigozzi F, Prinzi G (eds) Proceedings of the 4th Annual Congress of the European College of Sport Science. Rome, p14

Mader A, Heck H (1986) A theory of the metabolic origin of anaerobic threshold. Int J Sports Med 7 [Suppl 1]:45–65

Mader A, Heck H (1996) Energiestoffwechselregulation, Erweiterungen des theoretischen Konzepts und seiner Begründungen. Nachweis der praktischen Nützlichkeit der Simulation des Energiestoffwechsels. In: Mader A, Allmer H (eds) Computersimulation – Möglichkeiten zur Theoriebildung und Ergebnisinterpretation. Brennpunkte der Sportwissenschaft. Academia, St. Augustin

Mader A,Heck H, Hollmann W (1983) A computer simulation model of energy output in relation to metabolic rate and internal environment. In: Knuttgen J, Vogel A, Portmanns J (eds) Biochemistry of exercise. International Series on Sport Sciences, vol 13. Human Kinetics, Champaign, Ill.

Mast F, Elzinga G (1987) Heat production and oxygen consumption following contraction of isolated rabbit papilalary muscle at 20°C. In: Jacob R, Just H, Holubarsch C (eds) Cardiac energetics. Basic mechanism and clinical implications. Springer, Berlin Heidelberg New York, pp 86–92

McGilvery RW, Murray TW (1974) Calculated equilibria of phosphocreatine and adenosine phosphates. Biol Chem 249:5845–5850

McMillin JB, Pauly DF (1988) Control of mitochondrial respiration in muscle. Mol Cell Biochem 81:121 129

Meyer RA (1988) A linear model of muscle respiration explains monoexponential phosphocreatine changes. Am J Physiol 254:C548-C553

Meyer RA (1989) Linear dependence of muscle phosphocreatine kinetics on total creatine content. Am J Physiol 257:C1149-C1157

Mootha VK, Arai AE,Balaban RS (1997) Maximum oxidative phosphorylation capacity of the mammalian heart. Am J Physiol 272:H769-H775

Newsholme, EA, Start C (1973) Regulation in metabolism. Wiley, London

Nicholls DG, Ferguson SJ (1997) Bioenergetics 2. Academic Press, London

Nioka S, Argow Z, Dobson GP, Forster RE, Subramanian HV, Veech RL, Chance B (1992) Substrate regulation of mitochondrial oxidative phosphorylation in hypercapnic rabbit muscle J Appl Physiol 72:521–528

Parolin ML, Chesley A, Matsos M, Spriet LL, Jones NL, Heigenhauser GJF (1999) Regulation of skeletal muscle glycogen phosphorylase and PDH during maximal intermittent exercise. Am J Physiol 277:E890-E900

Rolfe DF, Brown GC (1997) Cellular energy utilization and molecular origin of standard metabolic rate in mammals. Physiol Rev 77:731–758

Rumsey WL, Schlosser C, Nuutinen EM, Robiolio M, Wilson DF (1990) Cellular energetics and the oxygen dependence of respiration in cardiac myocytes isolated from adult rat. J Biol Chem 265:15392–15399

Saborowski F, Usinger W, Albers C (1971) pH und CO2-Bindungskurve im Intrazellularraum der Skelett Muskulatur beim Hund. Pflugers Arch 328:121–134

Sahlin, K, Harris RC, Hultmann E (1975) Creatine kinase equilibrium and lactate content compared with muscle pH in tissue samples obtained after isometric exercise. Biochem J 152:173–180

Searle GL, Cavalieri RR (1972) Determination of lactate kinetics in the human analysis of data from single injection versus continuous infusion methods. Proc Soc Exp Biol 139:1002–1006

Soboll S (1995) Regulation of energy metabolism in liver. J Bioenerg Biomembr 27:571–582

Spriet LL, Söderlund K, Bergström M, Hultman E (1987a) Anaerobic energy release in skeletal muscle during electrical stimulation in men. J Appl Physiol 62:611–615

Spriet LL, Söderlund K, Bergström M, Hultman E (1987b) Skeletal muscle glycogenolysis, glycolysis, and pH during electrical stimulation in men. J Appl Physiol 62:616–621

Taylor DJ, Styles P, Matthews PM, Arnold DA, Gadian DG, Bore P, Radda GK (1986) Energetics of human muscles: exercise induced ATP-depletion. Magn Reson Med 3:44–54

Territo PR, Mootha VK, French SA, Balaban RS (2000) Ca^{2+} activation of heart mitochondrial oxidative phosphorylation: role of the F_0F_1-ATPase. Am J Physiol Cell Physiol 278: C423–C435

Thompson CH, Kemp GJ, Sanderson AL, Radda GK (1995) Skeletal muscle mitochondrial function studied by kinetic analysis of post exercise phosphocreatine resynthesis. J Appl Physiol 78:2131–2139

Trivedi B, Danforth WH (1966) Effect of pH on the kinetics of frog muscle phosphofructokinase. J Biol Chem 241:4110–4112

Veech LR, Lawson JWR, Cornell NW, Krebs HA (1979) Cytosolic phosphorylation potential. J Biol Chem 254:14, 6538

Wackerhage H, Hoffmann U, Esssfeld D, Leyck D, Mueller K, Zange J (1998) Recovery of free ADP, P_i, and free energy of ATP hydrolysis in human skeletal muscle. J Appl Physiol 85:2140–145

Wiseman RW, Kushmerick MJ (1997) Phosphorus metabolite distribution in skeletal muscle: quantitative bioenergetics using creatine analogs. Mol Cell Biochem 174:23–28

Williamson JR (1979) Mitochondrial function in the heart. Ann Rev Physiol 41:485–506

Wilson DF (1994) Factors affecting the rate and energetics of mitochondrial oxidative phosphorylation. Med Sci Sports Exerc 26:37–43

Wilson DF, Erecinska M, Schramm VL (1983) Evaluation of the relationship between the intra- and extramitochondrial [ATP]/[ADP] ratios using phosphoenol-pyruvate carboxykinase. J Biol Chem 258:10464–10473